

AD-A100 135

ROYAL AIRCRAFT ESTABLISHMENT FARNBOROUGH (ENGLAND)  
SOME REMARKS ON BUFFETING. (U)  
FEB 81 D G MABET  
RAE-TM-SIURCTURES-980

F/G 20/4

UNCLASSIFIED

DRIC-BR-78530

NL

AD  
Aero 1981

END  
DATE  
FILED  
7 81  
DTIC

UNLIMITED

TECH. MEMO  
STRUCTURES 980 ✓

LEVEL II

TECH. MEMO  
STRUCTURES 980

AD A100135

ROYAL AIRCRAFT ESTABLISHMENT

6

SOME REMARKS ON BUFFETING

by

10

D. G. Mabey

11

February 1981

DTIC  
SELECTED  
JUN 10 1981

12

35

E

9

Technical memo.

14

RAE-TM-STRUCTURES-980

18

DRIC

19

BR-78530

310450

LB

UNLIMITED

81 6 03 024

FILE COPY

X

ROYAL AIRCRAFT ESTABLISHMENT

Technical Memorandum Structures 980

Received for printing 5 February 1981

SOME REMARKS ON BUFFETING

by

D. G. Mabey

SUMMARY

Buffeting is defined as the structural response to the aerodynamic excitation produced by separated flows. The aerodynamic excitation produced by bubbles, vortices and transonic flows is discussed.

Different buffeting criteria for the wings of fighter and transport aircraft are developed. Methods of predicting the onset and severity of buffeting are reviewed. Some typical examples are discussed, in which improvements in wing buffeting are compared with changes in mean force measurements.

The first buffeting measurements on ordinary models in a cryogenic wind tunnel are analysed. The measurements confirm that cryogenic tunnels can separate Reynolds number and aeroelastic effects. The frequency parameter must be correct on the model if the aerodynamic excitation does not have a flat spectrum, as at vortex breakdown on a slender wing.

The violent periodic flows at transonic speeds recently observed on thick biconvex aerofoils are briefly reviewed and compared with solutions of the full Navier-Stokes equations.

This paper was prepared for the VKI lecture series "Unsteady airloads and aeroelastic problems in separated and transonic flows", to be given on 10 March, 1981 in Brussels.

Copyright

©

Controller HMSO London  
1981

LIST OF CONTENTS

	<u>Page</u>
NOTATION	3
1 INTRODUCTION	3
2 CLASSIFICATION OF WING FLOWS AND BUFFETING	4
3 EXPERIMENTAL METHODS	8
4 THEORETICAL METHODS	14
5 CONCLUSIONS	14
References	14
Illustrations	
Report documentation page	

Figures 1-35

inside back cover

Accession For	
NTIS GRA&I	<input checked="" type="checkbox"/>
DTIC TAB	<input type="checkbox"/>
Unannounced	<input type="checkbox"/>
JUL 1971	<input type="checkbox"/>
By	
Distribution Category	
Avail	Code
Dist	
A	I

NOTATION

$c$	wing chord (m)	$n$	frequency parameter $fL/V$
$C_B = C_B(M_s)$	buffeting coefficient - wing root strain signal/kinetic pressure (arbitrary units)	$p$	pressure fluctuation in a band $\Delta f$ at frequency $f$ ( $N/m^2$ )
$C_B'$ , $C_B''$	dimensionless buffeting coefficients defined in Equation (3) and (4)	$\bar{p}^2/q^2$	rms pressure fluctuations ( $N/m^2$ )
$C_L$	lift coefficient	$\bar{p}^2/q^2 = \int_{\log n=-\infty}^{\log n=\infty} nF(n)d(\log n)$	kinetic pressure $\frac{1}{2}\rho V^2$ ( $N/m^2$ )
$f$	frequency (Hz)	$R$	Reynolds number - based on aerodynamic mean chord
$F(n)$	contribution to $\bar{p}^2/q^2$ in frequency band $\Delta n$	$V$	free stream velocity (m/s)
$\sqrt{nF(n)}$	$p/q(\epsilon)^{1/2}$	$x$	distance from leading-edge (m)
$K$	transformation factor Equation (3)	$\alpha$	angle of incidence or angle of attack ( $^\circ$ )
$L$	typical dimension	$\epsilon$	analyser bandwidth ratio ( $\Delta f/f$ )
$l$	bubble length (m)	$\Lambda$	sweep angle ( $^\circ$ )
		$\rho$	free stream density ( $kg/m^3$ )

1 INTRODUCTION

We must first establish what we mean by buffeting. Buffeting is defined as the structural response to the aerodynamic excitation produced by separated flow. In the example sketched in Figure 1, there is a large area of separated flow on the wing. This provides the excitation which at a given point may be characterised by the rms level, the frequency spectrum (we shall see that the spectrum is often fairly flat at low frequencies), the degree of correlation in space and time, and the length scale. The pressure fluctuations excite a response of the structural modes which we call buffeting. The aircraft structure acts as a selective filter for the excitation so that spectra of buffeting always contain pronounced peaks at structural frequencies. In the example sketched in Figure 1 both the wing and the tailplane are excited. Rigid body modes may also be excited, such as "wing rocking", "wing dropping" or "nose slicing", but these are at much lower frequencies and can be regarded as aircraft handling problems, of great importance but outside the scope of this lecture. Buffet onset is often defined as the first appearance of a significant area of separated flow, although aerodynamicists often argue about how large the area must become before it is significant. (This is one of the uncertainties inherent in the theoretical methods for the prediction of buffet onset now being developed.) The onset of buffeting in flight is even more difficult to specify, for much of our present data are based on pilot impressions, which may be inaccurate if the pilot sits on or close to a node of the predominant modes being excited. Most pilots expect wing buffeting to provide a warning of more serious phenomena such as stall, pitch up or wing-drop, and are unhappy with aircraft which do not provide such a warning, unless an automatic visual or audio warning system is fitted.

The term buffeting was apparently first introduced into aeronautical literature when a structural failure occurred to the tail of a Junkers monoplane in 1930 (Ref 1). This failure was attributed by the British accident investigation to buffeting of the tailplane excited by flow separations on the wing. The flow separations on the wing were caused by an encounter with a severe gust and the German investigation attributed the accident directly to the structural failure of the wing caused by the gust (Ref 2). This incident emphasises again that buffeting often occurs in critical flight situations, when limit loads are being approached or when the aircraft is approaching lateral or longitudinal stability boundaries. (These early reports even include some discussion of the importance of correctly representing the aircraft geometry on the model and of the problems posed by testing at low Reynolds numbers. These issues are still important today.)

A consistent, dimensionless representation of excitation spectra is required when comparing measurements made at different flow densities and velocities. We shall adopt the notation suggested by T B Owen (Ref 3) and represented in Figure 2. Here we have a frequency parameter

$$n = fL/V ,$$

and an excitation level

$$p/q/\epsilon = \sqrt{nF(n)} .$$

### Buffeting Criteria for Fighter and Transport Aircraft

Figure 3 illustrates how buffeting criteria, expressed in terms of  $C_L - M$  boundaries, can influence the choice of wing loading for fighter and transport type aircraft. The boundaries presented for onset, light, moderate and heavy buffeting are based on some unpublished RAE measurements (Ref 4). (These boundaries are derived by a method outlined later.)

A typical fighter aircraft (with a wing leading-edge of sweep angle  $42^\circ$ ) will cruise well below the buffet onset boundary, but will frequently perform 5g manoeuvres which take it well beyond the buffet boundary to the moderate buffeting, or even to the heavy buffeting contour. For a fighter aircraft the moderate buffeting limit is sometimes taken as the highest level at which guns or missiles can be aimed successfully, whereas the heavy buffeting limit is that at which the aircraft becomes useless as a weapon platform, but is still controllable. For a fighter, frequent buffeting loads can seriously influence the fatigue life of the structure, for they are considerably larger than the loads caused by turbulence. The influence of the buffeting loads on the fatigue life of the new generation of advanced combat aircraft will need careful consideration. These aircraft can manoeuvre at higher lift coefficients and kinetic pressures than previous aircraft, without encountering rigid body modes such as wing dropping or nose slicing, because the separations are well controlled. However the pilot could be largely unaware of high frequency responses occurring in structural modes which could strongly influence the life of the airframe.

In contrast a typical transport aircraft (with the wing leading-edge of sweep angle  $27^\circ$ ) may cruise at about 0.1 in  $C_L$  below the buffet onset boundary. On infrequent occasions the aircraft may encounter a strong gust which carries the aircraft beyond the buffet boundary, right up to the moderate buffeting level. (The gust of 12.5 m/s selected in this example would have a wavelength of about 33 m (Ref 5)). The steady load achieved during the excursion into buffeting is probably more serious than the buffeting loads, which may be little larger than those associated with the atmospheric turbulence encountered during every flight.

Buffeting on fighter and transport aircraft only determines the extent of the penetration beyond the buffet boundary if there are no other handling limitations, such as wing rocking, wing dropping, pitch-up or stalling. We will return to this point later.

### 2 CLASSIFICATION OF WING FLOWS AND BUFFETING

A broad classification of wings with separated flows that excite buffeting will be useful as a framework for our discussion, even if the classification suggested is incomplete (Fig 4).

Wings with low angles of sweep are characterised beyond the buffet boundary at subsonic speeds by leading-edge or trailing-edge separations. These separations form bubbles on the wing which usually excite heavy buffeting. At transonic speeds the presence of strong shock waves nearly parallel with the leading-edge add to the difficulties of predicting the flow, so that we give this flow a prediction rating of 10. (These prediction ratings are arbitrary and not used in any calculations; an increase in prediction rating represents increased difficulty of prediction.) Swept wings are characterised by a combination of mixed flows (Ref 6) which are difficult to predict. The separated flows on a swept wing at transonic speeds may include shock waves (which vary in intensity across the span), bubbles (from the leading-edge or the trailing-edge) and vortices. Thus a small increase in Mach number may dramatically alter the position of a shock wave or the reattachment point of a bubble. Similarly an increase in unit Reynolds number or a change of the roughness band used to fix transition on the model in wind tunnel tests may completely alter the character of the shock wave/boundary layer interaction (References 7 and 8). These difficulties seem to justify a prediction rating for swept wings of 100; an even higher rating would be appropriate for a variable geometry wing.

Slender wings with sharp leading-edges are characterised by a simple vortex type of flow, which prevails over the complete speed range from subsonic to supersonic speeds. This unified type of flow is a powerful argument for the application for supersonic aircraft (Ref 9). The vortices, which produce significant non-linear lift, have a well defined, small scale structure and we shall see that they do not produce severe buffeting unless vortex breakdown occurs at high angles of attack outside the normal flight envelope. In addition the vortices on slender wings with sharp leading-edges are relatively insensitive to wide variations in Reynolds number. Hence slender wings are given a prediction rating of 1.

These prediction ratings are, of course, arbitrary, but they reflect real differences between the flows, which are now considered in greater detail.

#### Unswept Wings

The character of the excitation caused by leading-edge separation bubbles on unswept wings may be inferred (Ref 10) from the simplified model for a bubble suggested by Norbury and Crabtree in Reference 11 (Fig 5). In the constant-pressure region of the bubble, we would expect the excitation caused by low frequency fluctuations in the separation point to be relatively small, whereas in the reattachment region, where the rate of pressure recovery is high, the excitation should be much higher. Thus the excitation might be expected to reach a maximum in the middle of the reattachment region. These inferences from the mean static pressure distributions are broadly confirmed by the measurements, although the excitation attenuates both upstream and downstream of the reattachment region owing to the influence of the shear layer.

The spectrum of surface pressure fluctuations for a boundary layer approaching separation in an adverse pressure gradient may be divided into high-frequency and low-frequency components (Ref 12). The high-frequency pressure fluctuations are similar to those found under a boundary layer in zero pressure gradient (Ref 13) and are generated in the small scale inner region of the boundary layer associated with the law of the wall. The low-frequency pressure fluctuations are generated in the large-scale outer region

associated with the law of the wake, and increase in intensity as the outer region of the boundary layer thickens. Between separation and reattachment, measurements suggest that the low-frequency pressure fluctuations continue to increase steadily as the separated boundary layer thickens, until a point is reached where the mixing layer turns towards the surface and the mean pressure starts to increase. (Bradshaw has shown that the flow in the reattachment region is dominated by a rapid reduction in eddy size as the shear layer is divided into two halves. The lower half of the shear layer moves upstream from reattachment; the upper half moves downstream (Ref 14). It seems reasonable that this sudden reduction in eddy size should be accompanied by a sudden reduction in excitation at low frequencies.) Somewhere close to the reattachment point, the measurements for a wide range of bubble flows show a maximum value of the rms pressure fluctuation coefficient of

$$\bar{p}/q \text{ between } 0.10 \text{ and } 0.04 .$$

The spectra also show a marked similarity if the frequency parameter  $n$  is based on the bubble length  $l$ , for a peak pressure fluctuation is found when

$$n = fl/V = 0.5 \text{ to } 0.8 . \quad (1)$$

This probably implies a feed-back process between conditions at the reattachment and separation points. Equation (1) will be inappropriate when there is a strong, coherent disturbance in the wake (eg a Kármán vortex street) or if there are acoustic resonances (as there may be in cavities). The measured pressure fluctuations always cover a broad band of low frequencies, rather than a single discrete frequency as given by Equation (1), probably because the velocity of the eddies in the shear layer varies with the eddy size.

Leading-edge bubbles may be important for aircraft with sharp leading-edges, for which we have some good excitation measurements (Fig 6). Leading-edge bubbles were formed on the centre section of the Bristol 188 aircraft (Ref 15) and on a Venom aircraft with a sharp leading-edge (Ref 16). Figure 6 shows that the rms excitation at two points on the Bristol 188 increases gradually from separation ( $x/l = 0$ ), reaches a maximum of

$$\bar{p}/q = 0.10$$

just upstream of the reattachment point ( $x/l = 1.00$ ), and then decreases. The frequency parameter  $n$  based on the bubble length has a maximum at about  $n = 0.7$  and correlates the spectra quite well at  $x/c = 0.85$ , where most of the measurements are taken in the region of rapid pressure recovery ( $x/l = 0.94$ ). The peak level is about  $\sqrt{n}F(n) = 0.006$ . (The parameter  $n$  does not work so well at  $x/c = 0.50$ , where some of the measurements are taken in the constant steady pressure region ( $x/l = 0.56$ )). Measurements of pressure fluctuations on a Venom aircraft also conform to the general pattern shown in Figure 6(a) and show no significant variation in the rms pressure fluctuations or the spectra over the Mach number range from  $M = 0.3$  to  $0.6$ . Only a small Reynolds number effect on the low-speed pressure fluctuations was measured between the aircraft and a model (Ref 16). Some pressure fluctuation measurements on aerofoils with round leading edges (Ref 17) suggest similar rms levels and a peak frequency parameter of about 0.8 to 1.0.

Equation (1) helps us to discriminate between the excitation frequencies associated with long and short bubbles because of the large change in the bubble length between the two flows. A long bubble covers a significant area of the aerofoil chord and, from Reference 18, because

$$l/c \approx 0(1)$$

the pressure fluctuations will be at comparatively low frequencies which can excite the structural modes; eg for a long bubble on a wing with a chord of 3 m moving at 70 m/s, the excitation frequency would be

$$0 (12 \text{ Hz}) .$$

(Typical wing fundamental bending frequencies are 10 Hz for a small aeroplane and 2 Hz for a large aeroplane.) A short bubble only influences a small area of the wing, but, in addition, because

$$l/c \approx 0(0.01)$$

these pressure fluctuations will be at such high frequencies that they are unlikely to excite structural modes; eg for a short bubble on a wing with 3 m chord moving at 70 m/s, the excitation frequency would be

$$0 (1200 \text{ Hz}) .$$

Flight tests on the Venom with a sharp leading-edge (Ref 16), and the canard control of the XB-70 (Ref 19), showed that buffet onset corresponded with the formation of a long bubble. The buffeting then increased steadily as the bubble extended downstream, until the reattachment point approached the trailing-edge and the trailing-edge pressure diverged. This point corresponded with heavy buffeting. Hence the local pressure fluctuations within a long bubble must be quite strongly correlated.

The character of the excitation caused by a spoiler of height  $h$  (Fig 6(b)) closely resembles that caused by a leading-edge bubble. The excitation increases steadily from separation and reaches a maximum of

$$\bar{p}/q = 0.05$$

just upstream of reattachment. The peak frequency parameter  $n$  for the spoiler is about 0.9 in the experiments of Fricke, rather than 0.7 for the leading-edge bubble. The experiments of Fricke (Ref 20), in air, and of Greshilov (Ref 21), in water, give peak frequency parameters of about 0.9 and 0.8 although the bubble lengths are respectively 16 h and 5.5 h. The coincidence of the frequency parameters based on

bubble length confirms that this is a useful parameter for comparing the spectra of the pressure fluctuations generated by bubble flows.

The character of the rms pressure fluctuations and spectra caused by bubbles is largely independent of the origin of the bubble (Ref 10). Thus, in particular, the maximum pressure fluctuations occur just upstream of reattachment for:

- leading-edge bubbles,
- bubbles downstream of spoilers,
- bubbles downstream of steps,
- bubbles upstream of steps,
- bubbles downstream of sudden expansion in pipes,
- bubbles within shallow cavities (Fig 7).

Thus the data correlations presented in Reference 10 have application to a wide class of flows.

The prediction of the onset and severity of buffeting is of crucial importance at transonic speeds. In this speed range, the mixed subsonic/supersonic flows and the different regimes of shock/boundary layer interaction can modify the model for bubble flows described here, at least near the shock. However, downstream of the shock, an approximately constant average pressure is often observed in the separated flow region, followed by a rapid rise to reattachment. Coe's investigation (Ref 22) of the loads on launch vehicles included some measurements at subsonic and transonic speeds of the mean and fluctuating static pressures caused by a separation bubble downstream of a step in a body of revolution (Fig 8). Both the mean and fluctuating pressure distributions aft of the step correspond very well in general character with the low-speed pressure distributions over the complete speed range from  $M = 0.60$  to  $1.19$ , although the maximum fluctuating pressure falls steadily from

$$\bar{p}/q = 0.06 \text{ at } M = 0.80$$

to

$$\bar{p}/q = 0.03 \text{ at } M = 1.19 .$$

This fall in the pressure fluctuations is probably due to the improved stability of the mean bubble flow because of the reduction of upstream influence from the reattachment region as the region of supersonic flow expands. (The base-pressure fluctuations on a body of revolution also fall from subsonic to supersonic speeds and a similar explanation may be applicable (Ref 23)). The mean pressure distribution suggests that the length of the bubble does not change significantly from  $M = 0.60$  to  $1.19$  so that, within this speed range, there is probably no major change in the internal structure of the bubble.

The apparent universality of the pressure fluctuations caused by bubble flows at subsonic speeds is also well illustrated in Figure 8 which includes the pressure fluctuations measured (Ref 24) behind a two-dimensional step at  $M = 0.33$  as well as those measured (Ref 22) behind a step on a body of revolution at  $M = 0.80$ . The similarity at subsonic speeds between both the rms pressure fluctuations and the spectra for the two different experimental configurations and Reynolds numbers is good.

Recently some interesting measurements of the excitation on a two-dimensional lifting aerofoil at transonic speeds were made by Moss and Mundell and reported in Reference 25 (Fig 9). The condition selected for this aerofoil ( $M = 0.82$ ,  $\alpha = 6.7^\circ$ ) is just beyond buffet onset. Although the trailing-edge pressure has not yet diverged, there is a short separation bubble on the aerofoil (with a length of about  $l = 0.1 c$ ) immediately downstream of the shockwave. The position of the bubble was inferred from the shape of the mean pressure distribution, because it could not be seen in oil flow tests. (The interpretation of oil flow tests on two-dimensional aerofoils is often difficult because there are no telltale inflections in the streak lines as there are on swept wings).

The excitation measurements along the chord are presented for two frequency parameters

$$n = f_c/V = 0.08 \text{ and } 0.8 .$$

At a frequency parameter of  $n = 0.08$ , a typical value for wing structural modes, there is a large local increase in excitation in the vicinity of the shock wave. This local excitation decreases rapidly downstream of the shock wave but then shows a small local maximum in the vicinity of the reattachment region, before decreasing again. This variation in low-frequency excitation must be caused by the coupling of the shock wave motion (at separation) with the development of the bubble and with conditions at reattachment. In contrast, at a frequency parameter of  $n = 0.8$ , a typical value for wing panel modes, the excitation increases progressively downstream from the shock position, reaches a maximum close to the reattachment line and then falls rapidly as in the other bubble flows discussed in this section.

To find how the excitation develops, the angle of attack may be increased at constant Mach number. The separation bubble then extends rapidly towards the trailing-edge and the trailing-edge pressure diverges, while the shock wave starts to move upstream slowly. Thus the area of the aerofoil influenced by both the low frequency and high frequency excitation increases, and a progressive increase in buffeting would be expected. It should be noted that as the bubble extends rapidly in length from about  $l = 0.1 c$  to  $l = 0.5 c$ , the predominant bubble frequency parameter will fall from  $n = 8$  to  $n = 1.6$ , so that there should be a large increase in excitation in a frequency range centred on this lower value.

#### Swept Wings

Figure 10 shows the complex separated flow on a typical model with swept wings at a Mach number of  $0.80$  at low Reynolds number. These sketches illustrate some of the features which make buffet prediction difficult for swept wings and justify the prediction rating of 100 allotted in Figure 4. At buffet onset

there are at least three shockwaves on the wing and a small shock induced separation bubble (with a length of perhaps  $0.05 c$ ) immediately downstream of the strongest shock wave, which runs roughly parallel with the leading-edge. At moderate buffeting there are complex shock patterns on the wing, areas of separated flow and areas with attached flow having a strong spanwise velocity component. (Great care is always necessary to achieve an optimum transition fix for the boundary layer under high lift conditions like this at transonic speeds if large scale effects are to be avoided. The essential aim in the model test is to achieve the full scale boundary layer shape parameter,  $H$ , at the shock-wave/boundary-layer interaction. This aim can often be achieved by comparing the results of modern boundary layer calculation methods at model and full scale Reynolds numbers).

Pressure fluctuations are presented for a single point P on the wing; Figure 11 shows the variation of rms pressure fluctuations with the angle of attack. An attempt is made to explain this variation, but it is speculative because of the difficulty of discriminating between local events at P and what is happening simultaneously elsewhere on the wing. A local Mach number of 1.0 is reached at a small angle of attack at a point on the wing near the trailing-edge and close to the tip. A local region of supersonic flow then develops as the angle of attack increases. This supersonic region is terminated by a shock wave, which oscillates upstream and downstream. The pressure fluctuations at P first increase slowly with the angle of attack (point A,  $\alpha = 1.8^\circ$ ) because of the combined effect of the shock oscillation and the pressure fluctuations caused by an attached boundary layer growing under an increasingly adverse pressure gradient (Ref 12). As the terminal shock wave approaches and passes the transducer position (point B,  $\alpha = 5.0^\circ$ ) the pressure fluctuations increase rapidly; the major part of this increase must come from the shock wave oscillation. Shortly after point B the boundary layer separates at the terminal shock, and the terminal shock then starts to move forward and buffeting is detected by the wing-root strain gauges. (Thus the wing-root strain gauges give a measure of the integrated excitation on the wing). When the terminal shock moves upstream of the pressure transducer the local pressure fluctuations fall rapidly to a minimum at about  $\alpha = 6^\circ$  because the point P is no longer influenced directly by the shock oscillation. The pressure fluctuations then increase to a maximum (point C,  $\alpha = 7.2^\circ$ ), when the reattachment line crosses the pressure transducer, just as on the aerofoil (Fig 9). The local pressure fluctuations then decrease as the bubble extends downstream, although the wing buffeting, which is the response to the local excitation on the wing, continues to increase steadily from moderate to heavy.

The spectra of the pressure fluctuations provide additional information. Figure 12 shows that at point A, well below the buffet onset, the increase in pressure fluctuations is above the frequency range of wing modes. At the point B, with the terminal shock oscillating across the transducer, the peak pressure fluctuations become larger and move to lower frequencies, within the range of wing modes. At the point C, this peak is lower, because the shock is upstream of the transducer. However we notice at point C that there is an increase in pressure fluctuations at high frequencies ( $n > 0.5$ ). This may be associated with the separation bubble downstream of the shock. By analogy with the low-speed results, we might expect to find a second peak in the spectra at  $n = 5$  to 10 with this short length of bubble ( $l \approx 0.1 c$ ) but the present measurements did not extend much beyond  $n = 1.0$ .

This is obviously only a simplified account of the development of the excitation, using data from a single point on a wing. A complete description of the excitation all over a wing (including rms levels, spectra and correlations) is difficult to achieve. Extensive computing facilities are also needed to utilize this data to predict buffeting (3.0). Hence few measurements of excitation are currently available for swept wings at transonic speeds. However, we can learn a great deal about the wing behaviour from buffeting measurements, and these are discussed later.

#### Slender Wings

The fluctuating normal force measurements of Earnshaw and Lawford (Ref 26) (Fig 13) show that slender wings with sharp leading-edges can operate up to quite high angles of attack (and hence achieve reasonably high lift coefficients) without experiencing strong excitation. Although these tests were made at low Reynolds number ( $R = 0.2 \times 10^6$  to  $0.4 \times 10^6$ ), the flow characteristics of wings with sharp leading-edges are insensitive to wide changes in Reynolds number, primarily because the separation lines are fixed.

Recent measurements on the Concorde by BAC/Aerospatiale confirm that the level of excitation is light and almost identical with that measured on a 1/30 scale model (Ref 27) (Fig 14). Hence we may be confident that Reynolds number effects on the excitation of slender wing configurations with sharp leading-edges are insignificant.

The excitation is also light on slender wings with round leading-edges. However on slender wings with round leading-edges, large scale effects have been observed, particularly at subsonic speeds. A well documented example is the scale effects on the development of the leading-edge separations observed on the FD2 research aircraft (see References 28 and 29, and Figure 12 in Reference 30).

Although the level of excitation on slender wings is small, the level of buffeting attained is of interest because a slender-wing aircraft must fly above the buffet boundary on every take-off and landing, and thus acquire a large number of loading cycles during its operational life. The buffeting on rigid models of slender wings can be detected by sensitive semiconductor strain gauges (Ref 31). Measurements on two different rigid models conformed to the same pattern. Buffeting increases after the formation of the vortices and then reaches a plateau (Fig 15). This plateau is obtained because, although the area influenced by the vortices is increasing, the vortices are moving away from the wing. A sudden further increase in buffeting occurs when the vortex breakdown point moves across the trailing-edge, but it is unlikely that a slender wing aircraft would be required to operate in this region. An unusual feature of these buffeting measurements was that the third symmetric mode predominated, rather than the fundamental (as discussed later). Thus these measurements could not be used with confidence to predict the level of buffeting, quite apart from uncertainties about the appropriate damping coefficient. The solution found to this problem was to test an aero-elastic model for a rather similar configuration.

The buffeting on this aeroelastic model was readily detected by wire strain gauges (Ref 31), even though the tests were restricted to low equivalent airspeeds because of the danger of overloading and

destroying a valuable aeroelastic model. (Most aeroelastic models are designed for flutter testing under zero lift conditions). The buffeting on the aeroelastic model was also predominantly in the second and third structural modes, confirming the results for the rigid models. This response is probably caused by the excitation being localized to a comparatively small area under the vortices, rather than being distributed across the span as for unswept and swept wings. The level of buffeting extrapolated to full scale from this model was estimated to be small but just measurable. This prediction has recently been confirmed in flight.

In flight most of the buffeting is in the second and third structural modes. At the low values of EAS at which the aircraft flies above the buffet boundary there is little aerodynamic damping in these modes so that we may reasonably assume constant damping. The wing-tip acceleration A will then vary with  $V^2$  at a constant angle of attack. Hence the curve of

$$A/V^2 \text{ versus } \alpha$$

derived from the flight measurements at constant weight closely resembles that measured on the model (Fig 15) at constant kinetic pressure.

The level of buffeting has also been calculated by Mitchell (Ref 32), using as the excitation the pressure fluctuations measured at 14 points on the 1/30 scale model (Ref 27). Mitchell had to make rather sweeping assumptions about the correlations of the pressure fluctuations, and also to assume values of total damping appropriate to the motion, but he succeeded in predicting almost exactly the buffeting levels recently measured in flight.

Many readers will be disappointed that the correlation of the pressure fluctuations in these vortex flows has not been discussed. This primarily because there are so few correlation measurements available. The most complete set available to the author are those for a model of the BAC 221, a slender wing research aircraft. Figure 16 shows a typical example, with vortex breakdown about halfway between the apex of the wing and the trailing-edge (Ref 27). The contours of excitation have a maximum value underneath the point at which the vortex bursts. Using this point as reference we can then observe the correlation of the pressure fluctuations at the frequency selected. The clear impression given by all the contours of correlation is of a definite wave pattern. It is possible to show, by time delay techniques, that the contours are caused by the convection downstream of a fixed wave pattern associated with the vortex burst.

### 3 EXPERIMENTAL METHODS

Although the onset of flow separations (the buffet boundary) can be predicted by a combination of boundary layer methods and potential flow theory, adequate theoretical methods are not yet available to predict the aerodynamic excitation after separation. Hence the prediction of the severity of aircraft buffeting will continue to depend on model tests in wind tunnels, and recent improvements in these tests are considerable interest.

Three types of model tests to predict aircraft buffeting are discussed:

- (1) Ordinary wind tunnel models used to measure the unsteady wing-root strain in the first bending mode.
- (2) Ordinary wind tunnel models used to measure the unsteady pressure across the appropriate surface, and
- (3) Aeroelastic models (ie models designed with representative stiffness and inertia) used to measure unsteady responses.

The importance of using wind tunnels with low levels of flow unsteadiness is emphasised. Alternative methods of determining buffet onset are discussed.

#### Buffet Onset

In Reference 33 Huston et al suggested a method for predicting the onset of buffeting and flight buffeting loads from measurements of unsteady wing-root strain made on ordinary wind tunnel models with unswept and swept wings. Thus buffeting tests could be made simultaneously with routine force measurements. The similarity relations suggested are shown in Figure 17.

The method assumes that the reduced frequencies of the wing fundamental mode are about the same for the model and the aircraft, ie

$$f_{c, \text{model}} / f_{c, \text{aircraft}} \approx 1 .$$

In practice a variation in reduced frequency parameter from 0.7 to 1.6 seems to be accepted, at least for measurements of buffet onset (Ref 29), probably because the buffet excitation spectra are always comparatively smooth (eg Figure 12, Curves B and C). The measurement of unsteady wing-root strain is generally accepted as the most consistent and reliable method of assessing buffet onset from model tests (References 29, 34 and 35) and many tunnel/flight comparisons of buffet onset are available (References 29 and 35). There is generally a fair correlation between the tunnel and flight buffet onset boundaries over an extreme range of wing planforms and thickness distributions. Tunnel results obtained by this method are usually somewhat pessimistic, particularly at subsonic speeds, but are extremely useful for project studies and comparative tests. Reference 36 includes numerous examples of such comparisons.

Some recent buffet onset measurements (Ref 37) on a large half model are of particular interest, because the model achieved full scale Reynolds numbers. On this 42° swept wing scale effects were small and Fig 18 shows an excellent comparison between the tunnel and flight buffet onset boundaries.

The improvements in wing buffeting caused by the postponement or alleviation of flow separations can sometimes be associated with changes in the mean forces and pressures on the wing, particularly for low angles of sweepback where the buffeting is generally heavy. (For moderate or highly swept wings this is a much more difficult process. The term "kinkology" has been applied for these methods of determining improvements in buffet. Reference 38 includes some interesting examples). Thus Figure 19 shows that the slats which delay heavy buffeting on the 35° swept wing (Ref 39) also improve  $C_{L_{max}}$  from about 1.0 to 1.3. The slat also delays the divergence of the trailing-edge static pressure at a typical wing station ( $2y/b = 0.50$ ).

When dynamic wing buffeting tests are made in wind tunnels with low levels of flow unsteadiness the onset of buffeting is normally well defined. However if the flow unsteadiness at the wing fundamental frequency exceeds the levels specified in Reference 40, interpretation of the wing-root strain measurements may be difficult, and incorrect answers can be obtained. When the wing-root strain measurements are ambiguous a critical assessment of the overall forces may identify buffet onset. The examples which follow represent a bad failure of the dynamic method in some early tests in an unsteady tunnel ( $\sqrt{nF(n)} = 0.008$ ), and are not typical of what is readily achieved in a tunnel with low unsteadiness.

Figure 20 shows a comparison of the buffet onset boundary for a typical wing with low sweepback with two criteria for the onset of flow separations (Ref 29). The breaks in the  $C_D$  vs  $C_L^2$  curves correspond quite well with the onset of flow separations derived from surface flow visualisation. This boundary also compares fairly well with the buffet boundary at subsonic speeds ( $M < 0.80$ ) but at transonic speeds the buffet boundary is manifestly too high. In contrast the breaks in the  $C_L$  vs  $\alpha$  curves occur at such a high  $C_L$  over the complete Mach number range that they give too high a level for buffet onset. This observation is in accordance with the experiments of Ray and Taylor on a large number of wings (Ref 34). On a three-dimensional wing the initial onset of separation and loss of lift on one area of the wing may be associated with a compensating increase in lift on another area of the wing, so that there may be no breaks in the  $C_L$  vs  $\alpha$  curves at buffet onset. Although Bore has obtained some success with particular wings in using breaks in the  $C_L$  vs  $\alpha$  curves to obtain buffet onset boundaries (Ref 41), this method is not generally recommended.

Figure 21 shows the same buffet boundary compared with the trailing-edge pressure divergence boundaries. We see that every spanwise position on the wing gives a different divergence boundary, but that the boundary for  $2y/b = 0.82$  gives reasonably good agreement with the onset of flow separations at high subsonic and transonic speeds as Pearcey suggested (Ref 42). This station is recommended because many swept wings are designed so that the flow first separates at about  $2y/b = 0.80$ . Indeed at transonic speeds the combination of wing taper, leading-edge sweep and thickness distributions will often ensure the onset of flow separations in this area, unless flow separations can be deferred by modifications to the wing planform, the wing section or the wing twist distribution. For this wing the flow separations extend rapidly downstream from the leading-edge (at subsonic speeds) or from the terminal shock wave (at transonic speeds) and hence trailing-edge pressure divergence correlates reasonably well with buffet onset. The leading-edge separations on highly swept wings at transonic speeds generally extend rapidly to the trailing-edge so that trailing-edge pressure measurements can assist the interpretation of buffeting measurements on these wings (Ref 43). If the flow separations extend slowly downstream from the leading-edge, we have seen that trailing-edge pressure divergence will occur significantly later than buffet onset. (References 16 and 19).

Observation of the wing tip vortices can help to define the buffet onset boundary, if the initial flow separations are close to the wing tip. This technique has been rarely exploited, but during buffet tests in the RAE 3 ft x 3 ft Tunnel (Ref 29) close agreement was obtained on several models between the angle of attack at buffet onset derived from measurements of unsteady wing-root strain and the angle of attack at which the cores of the wing tip vortices disappeared from the schlieren image. When the wing flow is attached, the boundary layer near the wing tip is concentrated into the core of the wing tip vortex, and is clearly visible in a schlieren system with a horizontal knife-edge. However, if there is a separation on the outboard wing section, the vortex core rapidly diffuses and it is difficult to distinguish on the schlieren system. The change between these types of flow is well defined on the schlieren but not very well reproduced on photographs. The critical angle of attack is repeatable to  $\pm 0.1^\circ$  and small asymmetries between the onset of separation on port and starboard wings can be identified.

#### Severity of Buffeting

We must now return to the scaling of the buffeting loads from the model to the aircraft, which presents serious difficulties (Fig 17). Huston assumed that any differences between the mode shapes of the rigid model and the flexible aircraft would be insignificant and this is probably a fair assumption. He also assumed that it would be fairly easy to establish the total damping coefficient appropriate to the model and flight experiments but experience proves this hope is not well founded. Huston showed that for a given Mach number and angle of attack, if

$$\text{Wing-root strain} \propto \text{air density}$$

then the damping of the motion was predominantly structural and constant. Structural damping (generally denoted by  $g/2\% \text{ critical}$ ) seems to predominate on nearly all steel wind tunnel models (References 44 and 45) and remains constant from zero lift to heavy buffeting conditions. In contrast, if

$$\text{Wing-root strain} \propto (\text{air density})^{1/2}$$

Huston showed that the damping of the motion was predominantly aerodynamic. Huston suggested that this law would be followed in flight if the aerodynamic damping (generally denoted by  $\gamma \% \text{ critical}$ ) was unaltered by the onset of flow separations. However until recently there were few reliable flight experiments, and no conclusive tests on aeroelastic models in wind tunnels to verify this law. The measurements of Jones (Ref 46) originally suggested that in flight at constant density and velocity, but with varying angle of attack, the basic assumption of a constant damping coefficient equal to the attached flow value

was in error. Thus Figure 22(a) shows the variation of total apparent damping coefficient with normal force coefficient for a small fighter aircraft (Ref 46). At buffet onset the total apparent damping coefficient appeared to increase rapidly from its attached flow value, 3% critical, to 16% critical and then fall again to about 4% of critical in the region of moderate buffeting. No convincing explanation of this phenomenon was given and it was not known whether this behaviour was peculiar to this aircraft, or typical of most swept wing aircraft. A recent reappraisal of the estimates by Butler and Jones (Ref 47) suggests that at buffet onset the total apparent damping increases because of modal interference at low amplitudes. In this situation, the simple single degree of freedom analysis is inappropriate and misleading estimates can be obtained. In contrast, at moderate buffeting the fundamental bending mode generally predominates and realistic values of total damping are again obtained. This hypothesis explains the surprising variation in the previous estimates (Ref 46), which have been widely quoted. Fig 22 includes new estimates based on the original and additional measurements using refined techniques (Ref 47). The total damping estimates now only vary a little with normal force coefficients. This hypothesis could explain previous variations in apparent damping observed in other flight and tunnel tests, which have been analysed in a similar fashion.

A similar variation of total damping with lift coefficient has been derived at least once before (Ref 48) during wind tunnel buffeting tests of a rigid model over a limited Mach number range from  $M = 0.93$  to 1.00. Figure 22(b) shows that the structural damping of this model was low and the same for all configurations tested ( $g/2 = 0.4\%$  of critical damping). For the clean wing the total damping of the fundamental mode remained about 2% from low lift until well beyond buffet onset, then increased slowly to about 3% and then decreased again. (This variation is rather larger than we would expect for a rigid model, although Wornom and Davies observed a variation from 3% to 1.5% which could be related with the lift on the model (Ref 44). In contrast, for the same wing structure and frequency, but with the aerodynamics altered by the addition of bodies and fences, the damping started at low lift coefficients at the same level as the clean wing (2%) but then increased rapidly to 6% at buffet onset ( $C_L = 0.7$ ). The damping reached a maximum of 8.5% at  $C_L = 0.8$  and then fell to about 4% at  $C_L = 0.9$  to 1.0. The author of the original report thought that this change in damping was caused by the change in the flow produced by the wing modifications and not by any peculiar variation of structural damping. Figure 22(c) shows a similar variation of total damping for another improved configuration of the same wing at a Mach number of 0.98. Once again, a large increase in the total damping seems to occur before buffet onset. If variations of damping coefficient of this kind are going to occur in flight or tunnel experiments it will be impossible to utilize the simple relations for the severity of buffeting previously suggested (Fig 17).

Recently, Jones showed (Ref 49) that the non-dimensional aerodynamic excitation parameter appropriate to a flexible mode of vibration could be derived from measurements of buffeting response and total damping ratio. Subsequently this non-dimensional buffet excitation parameter in the first wing bending mode was derived from measurements made on wings of different materials, to give variations in response and damping, but under nominally identical free stream conditions (Ref 50). To test the scaling relationships implicit in the use of this non-dimensional buffet excitation parameter the flow required to excite the wing buffeting had to be relatively unaffected by a wide variation in Reynolds number and preferably unaltered in general character by a Mach number variation from subsonic to supersonic speeds. These conditions were satisfied by the choice of a slender wing with a well-ordered vortex flow (Ref 9), and accordingly a half-model of a delta wing, with a sharp leading-edge swept back 65°, was used. On this simple configuration a variation in the relative proportion of aerodynamic and structural damping at constant Reynolds number was obtained by testing two nominally identical wings, one of mild steel, and the other of magnesium alloy. These materials were selected because they had the same ratio of Young's modulus  $E$ , to density  $\rho_m$ . (Aluminum alloy also has the same value of  $E/\rho_m$  as steel and magnesium). Hence their natural frequencies were virtually identical and their mode shapes similar. Both wings could be tested over a wide range of free stream density,  $\rho$ , at constant Mach number, giving the same value of the ratio  $\rho/\rho_m$  for different combinations of  $\rho$  and  $\rho_m$ .

The idea of using geometrically similar models of steel and magnesium was suggested by a previous buffeting investigation (Ref 51). However the results of that investigation were inconclusive, possibly because the aerodynamic characteristics of the wing planform and section selected were sensitive to changes in Mach number and Reynolds number. (In that investigation the kinetic pressure  $q$  was varied by changing the Mach number at constant tunnel total pressure, and no tests were included at constant Mach number over a range of Reynolds number).

The results of the present investigation on the 65° delta wing configuration show that on the steel wing small variations in total damping ratio with free stream density can be detected. On the magnesium wing significantly larger variations in total damping ratio with free stream density are observed (Fig 23). When the total damping ratios are combined with the responses (given by the wing-root strain) a measure of the buffet excitation (or forcing function) is derived, and this is almost the same for both wings and independent of Reynolds number (Fig 24). The measurements extend well into the vortex breakdown region, and thus represent a useful extension of our knowledge of slender wing buffeting. (Earlier measurements of slender wing buffeting were limited by a load restriction on the aeroelastic model (Ref 31)). Fig 24 also includes the buffet excitation parameter measured by Butler and Spavins<sup>37</sup> on a typical fighter aircraft.

The wider implication of these tests is that it should be possible always to predict the buffet forcing function from tests of ordinary wind-tunnel models, as long as the total damping ratio is derived accurately. However if predictions for buffeting in flight are required, the total damping ratio measured during the model tests must be separated into the aerodynamic and structural components. This condition is somewhat restrictive, and implies that a wide free stream density variation (say 2/1) should be included for several Mach numbers of the model test programme.

Alternatively we may by-pass the uncertainties associated with the damping in flight and use the buffeting measurements on rigid wind tunnel models with constant damping to derive dimensionless buffeting coefficients which can then be compared directly with the buffet penetration achieved in flight (Ref 30) on aircraft for which we do not know the damping coefficients. Many assumptions are implicit in this method, but it works reasonably well. The basic hypothesis is that the tunnel unsteadiness (which must be known)

can be used as a given level of aerodynamic excitation to calibrate the model response at the wing fundamental frequency, and hence to derive buffeting coefficients from the buffeting measurements. These buffeting coefficients are a measure of the generalised force in the wing fundamental mode due to any distribution of pressure fluctuations on the wing. Past experience with nine aircraft models suggests that levels of buffeting coefficient obtained in this way can be identified appropriate to the maximum flight penetration of buffeting for both transport and fighter type aircraft. The method is illustrated by a typical example (Ref 29), the same model as discussed in Figure 20 and 21.

Figure 25 shows the curve of unsteady wing-root strain signal at the wing fundamental frequency,  $f_1$ , plotted against angle of attack. If these signals are divided by the appropriate kinetic pressure  $q = \frac{1}{2} \rho V^2$ , we have, if the flow is insensitive to changes in Reynolds number.

$$\text{Wing-root strain signal}/q = C_B(M, \alpha) \quad (2)$$

where  $C_B(M, \alpha)$  is a dimensional function of Mach number  $M$  and is independent of  $q$  at a given  $M$  and angle of attack, the total damping of the wing fundamental mode being constant (Ref 45). Before the onset of flow separation on the model, most of the curves in Reference 29 and numerous tests in other wind tunnels (Ref 34) show that  $C_B(M, \alpha)$  is constant and equal to  $C_B(M, \alpha = 0)$ . This is the portion of the model response caused by the tunnel unsteadiness  $\sqrt{nF(n)}$  at the appropriate Mach number and the same frequency  $f_1$ . We now scale all the measurements so that the level  $C_B(M, \alpha = 0)$  represents the tunnel unsteadiness and the model response to that unsteadiness. Thus

$$C'_B(M, \alpha = 0) = \sqrt{nF(n)} = 1/K \quad . \quad C_B(M, \alpha = 0) \quad (3)$$

where  $K$  is a constant scaling factor. The subsequent increases in  $C'_B(M, \alpha)$  as the angle of attack increases gives a measure of the integrated pressure fluctuations arising from the wing buffet pressures and of the model response to this excitation. Having used the tunnel unsteadiness  $\sqrt{nF(n)}$  to establish a datum buffeting scale, this signal must now be subtracted to give the true buffeting level in the absence of tunnel unsteadiness. If the tunnel unsteadiness does not exceed the criteria in Reference 40 there should be no correlation between the tunnel unsteadiness and the wing buffeting and so we can calculate a corrected buffeting coefficient

$$C''_B(M, \alpha) = \sqrt{C'_B(M, \alpha)^2 - C'_B(M, \alpha = 0)^2} \quad . \quad (4)$$

The angle of attack at which  $C''_B(M, \alpha)$  first differs from zero is buffet onset. Contours of buffeting coefficients are then readily obtained as a function of Mach number and angle of attack or lift coefficient. For the seven fighter aircraft models heavy buffeting corresponds with

$$C''_B = 0.012 \text{ to } 0.016$$

For fighter aircraft there is considerable scatter from the flight buffet onset boundary to the  $C_B = 0.004$  contour. Hence for fighter aircraft the following buffeting criteria are suggested:

Buffet onset	$C'_B = 0$
Light buffeting	$C'_B = 0.004$
Moderate buffeting	$C'_B = 0.008$
Heavy buffeting	$C'_B = 0.016$

For the two transport aircraft models the buffeting limit corresponds with  $C'_B = 0.006$ .

Figure 26 illustrates a test of this hypothesis for a fighter aircraft. The model was similar to the one considered in Figure 25 but the tunnel unsteadiness was much lower ( $\sqrt{nF(n)} = 0.002$ ) and the Reynolds number much higher ( $R \approx 4 \times 10^6$ ). Buffet onset in the new flight tests (carefully derived from wing-tip accelerometers) agrees well with the light buffeting contour.

$$C''_B = 0.004$$

and the maximum flight penetration corresponds with the heavy buffeting contour

$$C''_B = 0.016 \quad .$$

Figure 27 shows sketches based on typical oil flow photographs taken on this model at Mach numbers of 0.70 and 0.90 at the light, moderate and heavy buffeting levels, and we note the progressive development of the areas of separated flow as the buffeting coefficient increases.

The correlations established between buffeting contours and maximum flight penetration are somewhat surprising because it might reasonably be expected that the severity of buffeting in flight would be based on the dimensional level of vibration (either estimated by the pilot or measured by an accelerometer), rather than a dimensionless buffeting coefficient. There are two alternative explanations for the correlations established. Either:

- (1) the severity of wing buffeting is not really the limiting factor so that pilots of fighter or strike aircraft tend to fly right up to handling boundary, such as pitch-up, stalling or wing dropping. This handling boundary might coincide with the heavy buffeting contour. Or
- (2) the pilot may instinctively include in his assessment of buffeting a 'q' factor, as he tends to do in the application of steady loads to the aircraft.

If he does introduce a 'q' factor, pilot-defined boundaries for light, moderate and heavy buffeting at constant altitude would tend to be uniformly spaced above the buffet onset boundary where Mach number effects are small, and would correspond with constant values of pressure-fluctuation coefficients measured

in the tunnel and hence of buffeting coefficients,  $C_B$  (see Figure 16 for the Venom aircraft with a sharp leading-edge).

The pilots of transport aircraft generally sit further from the nodal points of the wing fundamental mode than do pilots of fighter or strike aircraft and would not wish to approach a handling boundary, even if sufficient thrust were available. Thus for transport aircraft the maximum penetration coefficient  $C_B' = 0.006$  seems more reasonable than the value of 0.016 for fighter aircraft. This limit for maximum flight buffet penetration for transport aircraft of  $C_B' = 0.006$  is based on measurements for only two models at low Reynolds numbers and may need to be revised as additional tunnel/flight comparisons become available for this class of aircraft.

The heavy buffeting contour can be given a general physical significance because the buffeting coefficient ought to be of the same magnitude as the fluctuating normal force coefficient if the flow over most of the wing is separated and the excitation is well correlated across the wing. The measurements of Polentz on aerofoils (Ref 52) show a maximum normal force coefficient at low frequencies of about 0.010 to 0.020 which brackets the heavy buffeting contour of 0.016. Similarly Figure 13 shows that the maximum fluctuating normal force coefficient at a particular low frequency parameter  $n = 0.05$  for a family of slender wings varies from about  $\sqrt{nG(n)} = 0.008$  to 0.010 for  $\Lambda = 45^\circ$  to  $\sqrt{nG(n)} = 0.014$  to 0.019 for  $\Lambda = 70^\circ$ . These high values of normal force coefficient are obtained when vortex breakdown occurs on the wings irrespective of the details of the vortex flow (Ref 26).

Aircraft such as the Harrier, in which the spanwise development of flow separations is carefully controlled, achieve appreciably higher heavy buffeting coefficients than previous aircraft. This fact could have important implications for the structural loading of such aircraft (Ref 53, Section 3.1.3).

One application of this method utilized buffeting measurements made by Hanson on an aeroelastic model of a variable geometry fighter aircraft; the original report repays careful study (Ref 54). The aeroelastic model was tested in Freon 12 in the NASA Langley Transonic Dynamics Tunnel. The model was flown on wires and achieved an almost exact duplication of the aircraft mode and dampings for the different wing sweep angles. As expected, the response measured by the wing-root strain bridge was predominantly in the wing fundamental mode, at about 16 Hz model scale (Figure 8a of Reference 54), and the damping was predominantly aerodynamic. (The advantage of using correctly scaled aeroelastic models for buffeting tests is that the response in modes other than the wing fundamental bending can be measured accurately. Thus in Hanson's tests the tail response and fuselage vertical bending were measured. Hence the buffet excitation parameter (Refs 49 and 50) can also be derived for these widely differing modes).

Figure 28 shows a comparison of the buffeting contours derived from the model tests and the buffet onset and maximum penetration achieved in flight. In the tunnel tests the maximum penetration was not limited by wing buffeting, but instead either by a limiting tail deflection (the aeroelastic model must fly trimmed) or by a roll instability which the "pilot" could not control. Similarly in flight no manoeuvres were aborted due to the severity of buffeting, but only due to the attainment of the "g" and "i" limits mentioned in the report. For  $\Lambda = 26^\circ$  and  $50^\circ$  the flight buffet onset boundary agrees fairly well with the buffet onset contour  $C_B' = 0$  derived from the tunnel tests. For  $\Lambda = 70^\circ$  the flight buffet onset boundary is between the buffet onset contour  $C_B' = 0$  and the light buffeting contour  $C_B' = 0.004$ . Above buffet onset the flight and tunnel contours look similar and support the broad conclusion that maximum flight penetration would have corresponded fairly well with the heavy buffeting contour  $C_B' = 0.016$ , if this could have been achieved on the aeroelastic model. Even with the severe restrictions applied to the aeroelastic model by the tail deflection and the roll instability, maximum levels of  $C_B' = 0.010$  and 0.013 were achieved for  $\Lambda = 26^\circ$  and  $70^\circ$  respectively.

These results from an aeroelastic model flown on wires may reasonably be viewed as a severe, and yet fairly satisfactory, test of the hypothesis originally advanced in Reference 30 on the basis of tests on ordinary wind tunnel models supported by stings. It should be noted that buffeting tests on an ordinary sting-supported model of the aircraft would not have been limited by tail loads or a roll instability, and could probably have been made at higher Reynolds numbers. (The test Reynolds numbers quoted on page 10 of Reference 54 are in fact Reynolds numbers/ft so that the model Reynolds numbers are comparatively low, although this did not spoil the buffeting measurements).

It is interesting to note that in both the flight and tunnel tests reported in Reference 54 rapid increases in angle of attack excited less severe buffeting than slow increases in angle of attack. This effect has been noticed previously in flight tests of other combat aircraft. Although part of the delay can be attributed to the finite time taken by the structure to respond to the aerodynamic excitation (as discussed by Zbrozek and Jones in Reference 5), there is some evidence that there may well be, in addition, a transient effect on the development of the flow separations, if the rate of change of the angle of attack is high.

Buffeting measurements have also been made on a model of composite construction which represents the static bending and torsional stiffness of an aircraft project, but not the inertia distribution (Ref 55). Although this composite model was not a full aeroelastic model, having unrepresentative frequency parameters, it was more representative of the aircraft than the solid aluminium model tested for comparison. The composite model provided useful advance warning of a "torsional buzz" phenomenon subsequently observed in flight, which lies in the "no man's-land" between buffeting and flutter, and which did not occur on the solid model. There is still some doubt as to precisely how the pressure fluctuations on the wing couple with the torsional vibration, which is only observed with a leading-edge sweep angle of  $27.2^\circ$  in a small region about a Mach number of about 0.70 and an incidence of  $9^\circ$  (Ref 55, Fig 17). In some unpublished tests on an ordinary, steel wind tunnel model with almost the same geometry a large discrete excitation was observed in the same region at the same frequency parameter, although there was no structural mode on the model at that frequency.

Recent research on ordinary wind tunnel models has confirmed that in general the wing bending does not influence the measured oscillatory pressures when the flow is separated. (This may be seen directly from Figs 16 to 19 of Ref 56 or inferred from the buffeting measurements of Ref 50). The unsteady

pressures measured on ordinary wind tunnel models provide a useful indication of any unusual discrete excitation in the spectrum (as occurs with the circular cylinder). These pressures may, in principle, be integrated to give the total excitation (Ref 57). However the aircraft response can only be calculated with some additional assumption about the total damping in the mode. Hence most future predictions of the severity of buffeting will continue to be made from accelerometer or wing-root strain measurements, using either the buffet excitation parameter (Ref 49) or buffeting coefficients (Ref 30).

#### Buffeting Tests in Cryogenic Wind Tunnels

Kilgore et al have shown that the problems caused by static aeroelastic distortion in conventional wind tunnels should be much less severe in cryogenic wind tunnels (Ref 58). In cryogenic tunnels the kinetic pressure may be held constant for a constant total pressure while the Reynolds number is increased at constant Mach number by reducing the total temperature. This is an attractive concept for obtaining high Reynolds numbers at transonic speeds, and offers many advantages for buffeting tests on ordinary wind tunnel models (Ref 59). Recently Boyden has made some buffeting measurements (Ref 60) in the NASA Langley 0.3 m transonic cryogenic tunnel on two solid aluminium alloy wings (Fig 29). The preliminary results from the wing-root strain gauges on the 65° delta wing are directly comparable with the measurements already discussed (Figs 23 and 24) and are of great interest. In the subsequent figures, based on Boyden's data, the steady and unsteady signals from the wing-root strain gauges are divided by the kinetic pressure  $q$ , to form: a steady bending moment coefficient =  $\bar{C}_B$ , and an unsteady bending moment coefficient =  $C_B$ , exactly as in equation (2). Most of the unsteady bending moment response is at the fundamental bending frequency of 500 Hz at 300K. The small increase in frequency at the lower total temperature is caused by the increase in Young's modulus. These tentative comments by the author may stimulate further discussion of the technique.

Fig 30 shows how both bending moment coefficients vary with angle of incidence for a constant total pressure ( $p_t = 1.2$  bar), two total temperatures (300 and 110K) and a Mach number of 0.35. Now the kinetic pressure is the same at both total temperatures (Ref 58), so that the static aeroelastic distortion is identical for a given load. The steady bending moment coefficients,  $\bar{C}_B$ , are precisely the same at both total temperatures, confirming that scale effects are negligible on this highly swept slender wing over a wide range of Reynolds number. Before vortex breakdown the unsteady bending moment coefficients,  $C_B$ , are almost identical, despite the small change in frequency. This indicates that the excitation spectrum (due to the vortices and the tunnel unsteadiness) is relatively flat. In marked contrast, immediately after vortex breakdown the buffeting coefficients are quite different. The response is much higher at the higher frequency parameters obtained at the lower temperature. This increase in response with frequency parameter is consistent with the excitation measurements of Keating<sup>27</sup> on a similar planform (see spectrum of excitation in Fig 34). The large increase in response after vortex breakdown cannot be attributed to a decrease in the total damping coefficient, for this is estimated to increase from 1.3% to 1.6% of critical (due to the variation in aerodynamic damping) as the temperature is lowered from 300K to 110K.

Fig 31 shows buffeting measurements at 300K for  $M = 0.35$ . For a given incidence the steady bending moment coefficients decrease as the kinetic pressure increases because of static aeroelastic distortion. The change cannot be attributed to the variation in Reynolds number because this is precisely the same as in Fig 30; comparison of Figs 30 and 31 thus strongly supports the claim that cryogenic tunnels can easily separate Reynolds number and aeroelastic effects (Ref 58). In contrast with Fig 30, the buffeting coefficients in Fig 31 only vary a little after vortex breakdown because the frequency parameter is constant. The buffeting coefficients vary a little with kinetic pressure both at low incidences and after vortex breakdown. This small variation is consistent with the estimated small variation in the damping coefficient from 1.4% to 1.6% of critical (due to the variation in aerodynamic damping).

Fig 32 shows the effect of an increase in Mach number from 0.21 to 0.35. These special measurements are made at a constant frequency parameter (obtained by using a constant velocity of 73 ms) and at constant kinetic pressure (obtained by using a constant density). When these two parameters are constant, the aerodynamic damping, proportional to the product of density  $\times$  velocity, is constant. The steady bending moment coefficients increase rapidly with Mach number; the increase in bending moment coefficient looks appreciably larger than the expected increase in lift-curve slope. In contrast, the buffeting coefficients are virtually identical both before and after vortex breakdown, despite the difference in Mach number and the corresponding differences in the steady bending moment coefficients. The excellent agreement between both sets of buffeting coefficients after vortex breakdown is a direct consequence of maintaining a constant frequency parameter, and, to a lesser degree, of maintaining constant total damping (aerodynamic + structural), estimated to be 1.6% of critical. The importance of maintaining the correct frequency parameter in a buffeting test in a cryogenic wind tunnel was stressed previously (Ref 59).

The difficulty of achieving low structural damping and significant aerodynamic damping during buffeting tests on ordinary wind tunnel models has long been appreciated (Refs 44, 51 and 50). Most of the structural damping on an ordinary wind tunnel model is caused by friction between the wing and the root fixing. As long as both the wing-root and the attachment are at the same temperature and of the same material, the friction should be unchanged in a cryogenic wind tunnel test. Then there would be no *a priori* reason for a change in structural damping coefficient with total temperature. The wind-on structural damping coefficient inferred from the present buffeting measurements (Fig 31) is about 12% critical, which is typical of an ordinary wind tunnel model. The wind-off measurement is only about 0.3% critical at ambient conditions. The aerodynamic damping coefficient was estimated theoretically (Ref 50).

The aerodynamic damping obtained in a buffeting test at constant Mach number and total pressure in a cryogenic wind tunnel is  $1/T_t$  (Ref 59). Hence the proportion of aerodynamic to structural damping will increase at cryogenic temperatures. This will improve the scaling of the aerodynamic damping ratio from model to full scale (Ref 59).

Some preliminary measurements of the total damping coefficients derived from the power spectra of the wing-root strain measurements<sup>60</sup> have been added in proof; these measurements are in fair agreement with the estimates (Fig 33).

Fig 34 shows the spectrum of the excitation measured<sup>27</sup> at vortex breakdown for the same conditions as Fig 16. Although the geometry of the BAC 221 was appreciably different from a 65° delta wing, it is known that the flows on both wings are broadly comparable. The large increase in excitation from a frequency parameter,  $f_{c_0}/V$ , from 0.8 to 1.4 is consistent with the increase in response shown in Fig 30. The spectrum of the excitation measured on unswept rectangular wings is generally flatter than that shown in Fig 34, and hence Boyden's buffeting measurements<sup>60</sup> on the other wing shown in Fig 29 are not sensitive to the variation in frequency parameter.

#### 4 THEORETICAL METHODS

Numerical methods have been developed now to solve the full Navier-Stokes equations for two-dimensional flows, with a choice of different turbulence models. Chapman has given a comprehensive review of these interesting recent developments (Ref 61).

These methods can predict the unusual periodic flows sometimes generated by shock induced separations on aerofoils over a narrow range of Mach numbers at transonic speeds. The predicted and observed flows on an 18% thick biconvex aerofoil at zero incidence are discussed in Refs 62 and 63. Fig 35 shows a recent example of such a periodic flow at  $M = 0.85$  on a 14% thick biconvex aerofoil at zero incidence. The flow predicted by L Levy of NASA Ames is in excellent agreement with the measurements made at RAE, both with respect to the lift and moment fluctuations and the frequency (Ref 64). These large periodic pressures are developed without any aerofoil motion.

On a flexible wing, excitation as large as this could produce serious buffeting, if the frequency coincides with a structural mode. The frequency parameter,  $f_c/V$ , lies in the range from 0.1 to 0.2 and thus the wing torsion or overtone bending modes are more likely to be excited than the first bending mode.

Chapman has remarked that so far these methods have only predicted the pressure fluctuations caused by low frequency, large scale flow separations. The methods have not succeeded in predicting the random pressure fluctuations in the normal excitation spectrum, caused by the smaller eddies. The methods are not yet applicable to three-dimensional flows.

#### 5 CONCLUSIONS

The main themes relate to Figure 4, and can be reiterated as follows: (1) For bubble flows, which occur in many different situations, the largest excitation is found just upstream of the reattachment point; (2) For slender wings with sharp leading-edges the buffeting is light, but just measurable, exactly as predicted from wind tunnel tests 8 to 10 years in advance of flight; and (3) For swept wings the complex nature of the flows and wing performance assessment are best examined by buffeting measurements on rigid models, despite their limitations.

Recent developments include the use of ordinary models in cryogenic wind tunnels (to predict the aircraft response) and the numerical solution of the full Navier-Stokes equations (to predict the aerodynamic excitation in periodic flows). Both methods may ultimately be of interest in evaluating aircraft performance beyond the buffet boundary.

#### REFERENCES

- 1 - Technical Report on the Accidents Investigation Sub-Committee on the accident to the Aeroplane G-AAX at Shepperton, Kent on 21 July 1930, RM 1360, January 1931.
- 2 Blenk, H. "Vorbericht über die Abreissen der Flügeloberflächen und deren Verhinderung", Zeitschrift für Fliegerwesen und Luftfahrt, ZFM 24, 1943, 21-24, also English translation NACA TM 669.
- 3 Owen, T.B. "Comparison of Pressure Fluctuation Measurements Employed in the RAE Low Speed Wind Tunnel", AGARD Report 172, 1958.
- 4 Mabey, D.G., Moss, G. RAF unpublished.
- 5 Zbrozek, J.K., Jones, J.G. "Sound and Vibration in Wings", Journal of Sound and Vibration, Vol.5, No.2, pp.197-214, 1967.
- 6 Rogers, E.W.F. "An Introduction to the Flow About Planes Supt-Buck Wings at Transonic Speeds", Journal of Royal Aeronautical Society, Vol.64, pp.449-464, 1960.
- 7 Green, J.E. "The Importance of Viscous-Inviscid Interactions at Transonic Speeds, and their Dependence on Reynolds Number", AGARD CP 83, 1971.
- 8 Blackwell, J.A. "Preliminary Study of the Effects of Reynolds Number and Boundary Layer Transition Location on Shock Induced Separation", NASA TN D 5003, 1969.
- 9 Klichemann, D., Weber, J. "An Analysis of some Performance Aspects of Various Types of Aircraft Designed to Fly over Different Range at Different Speeds", AGARD CP 83, 1971.
- 10 Mabey, D.G. "Analysis and Correlation of Data on Pressure Fluctuations in Separated Flow", AIAA Journal, August/September 1972.
- 11 Norbury, J.F., Crabtree, L.F. "A Simplified Model of the Incompressible Flow past Two-Dimensional Aerofoils with a Long Sudden Type of Separation", RAE TN Aero 2352, June 1955.
- 12 Bradshaw, P. "Turbulence, Method and Pressure Fluctuations in Turbulent Boundary Layers", NPL Aero Report 1172, October 1965, (Also published as ARC 27338).

- Str 980.
- 13 Lilley, G.M. On Wall Pressure Fluctuations in Turbulent Boundary Layers, ARC 24241, November 1962.
  - 14 Bradshaw, P. Wong, F.Y.G. The Reattachment and Relaxation of a Turbulent Shear Layer. Journal of Fluid Mechanics, Vol.52, part p 1, pp.113-135, 1972.
  - 15 Lawford, J.A. Beauchamp, A.R. Low Speed Wind Tunnel Measurements of Pressure Fluctuations on the Wing of a Twin Jet Aircraft (Bristol 188), ARC R&M 3551, 1968.
  - 16 Rose, R. Flight and Tunnel Measurements of Pressure Fluctuations on the Upper Surface of the Wing of a Venom Aircraft with a Sharp Leading-Edge. ARC CP 1032, November 1967.
  - 17 Heller, H.H. Bliss, D.B. Incipient Stall Detection through Unsteady Pressure Monitoring on Aircraft Wings, Journal of Aircraft, Vol.9, No.2, pp.186-188, February 1972.
  - 18 Crabtree, L.F. The Formation of Regions of Separated Flow on Wing Surfaces, Pt II Laminar Separation Bubbles and the Mechanism of the Leading-Edge Stall, RAE Report Aero 2578, July 1957, also in Pt 2 of ARC R&M 3122, 1959.
  - 19 Jenkins, J.M et al Flight Measurements of Canard Loads, Canard Buffeting and Wing Tip Hinge Moments on the XB70 Aircraft Including Comparisons with Predictions, NASA TN D 5359, August 1969.
  - 20 Fricke, F.R. Stevenson, D.C. Pressure Fluctuations in a Separated Flow Region, Journal of the Acoustical Society of America, Vol.44, No.5, pp.1189-1201, November 1968.
  - 21 Greshilov, E.M. Evutshenko, A.V. Spectral Characteristics of the Wall Pressure Fluctuations Associated with Boundary Layer Separation Behind a Projection on a Smooth Wall, Soviet Physics - Acoustics, Vol.15, No.1, pp.29-34, July-September 1969.
  - 22 Coe, C.F. The Effects of Some Variations in Launch Vehicle Nose Shape on Steady and Fluctuating Pressures at Transonic Speeds, NASA TM X 646, March 1962.
  - 23 Mabey, D.G. Some Measurements of Base Pressure Fluctuations at Subsonic and Supersonic Speeds, RAE TR 70 148, August 1970, (also published as ARC CP 1204, 1972).
  - 24 Mohsen, A.M. Experimental Investigation of the Wall Pressure Fluctuations in Subsonic Separated Flow. Boeing Co, Report D6-17094, AD669214, January 1967.
  - 25 Moss, G.F. Mundell, A.R.G. RAE - unpublished.
  - 26 Earnshaw, J.A. Lawford, J.A. Low Speed Wind Tunnel Experiments on a Series of Sharp-Edge Delta Wings, R&M 3424, August 1964.
  - 27 Keating, R.F.A. RAE - unpublished.
  - 28 Dee, F.W. Nicholas, O.P. Flight Determination of Wing Flow Patterns and Buffet Boundaries for the Fairey Delta Aircraft at Mach numbers between 0.4 and 1.3 and Comparison with Wind Tunnel Tests, R&M 3482, 1964.
  - 29 Mabey, D.G. Comparison of Seven Wing Buffet Boundaries Measured in Wind Tunnels and In Flight, ARC CP 840.
  - 30 Mabey, D.G. An Hypothesis for the Prediction of Flight Penetration of Wing Buffeting from Dynamic Tests on Wind Tunnel Models, ARC CP 1171, 1971.
  - 31 Mabey, D.G. Measurements of Buffeting on Slender Wing Models, ARC CP No.954, 1967.
  - 32 Mitchell, C.G.B. Calculations on the Buffeting on a Slender Wing Aircraft at Low Speeds, Proceedings of the Symposium on Structural Dynamics, Loughborough University, March 1970.
  - 33 Huston, W.B. A Study of the Correlation between Flight and Wind Tunnel Buffet Loads, AGARD Report 121, April 1957, (Also published as ARC 20704).
  - 34 Ray, E.G. Taylor, R.T. Buffet and Static Aerodynamic Characteristics of a Systematic Series of Wings Determined from a Subsonic Wind Tunnel Study, NASA TN D 5805, 1970.
  - 35 Hollingsworth, E.G. Cohen, M. Comparison of Wind Tunnel and Flight Test Techniques for Determining Transonic Buffet Characteristics on the McDonnell Douglas F-4 Airplane, AIAA Paper No 70-584, 1970.
  - 36 Anon The Effects of Buffeting and other Transonic Phenomena on Manoeuvring Combat Aircraft, AGARD AR-82, July 1975.
  - 37 Butler, G.F. Spavins, G. Preliminary Investigation of a Technique for Predicting Buffet Loads in Flight from Wind-Tunnel Measurements on Models of Conventional Construction, AGARD CP 204.

- 38 John, H. *Critical Review of Methods to Predict the Buffet Capability of Aircraft*, AGARD Report R623, September 1974.
- 39 Moss, G.F. Haines, A.R. Jordan, R. *The Effect of Leading-Edge Geometry on High Speed Stalling*, AGARD CP 102, November 1972, (Also published as RAE TR 72099).
- 40 Mabey, D.G. *Flow Unsteadiness and Model Vibration in Wind Tunnels at Subsonic and Transonic Speeds*, ARC CP 1155, 1971.
- 41 Bore, C.L. *Post Stall Aerodynamics of the "Harrier" CT*, AGARD CP 102, November 1972.
- 42 Pearcey, H.H. *Simple Methods for the Prediction of Wing Buffeting Results from Bubble Type Separations*, NPL Aero Report 1024, June 1962.
- 43 Mayes, J.F. Lores, M.E. Barnard, H.R. *Transonic Buffet Characteristics of a 60 Degree Sweep Wing with Design Variation*, AIAA Paper No 69-793, (1969), (Also Journal Aircraft I, pp.523-530 (1970)).
- 44 Davis, D.D. Wornom, D.E. *Buffet Tests of an Attack Airplane Model with Emphasis on Data from Wind Tunnel Tests*, NACA RM L 57, H13, February 1958.
- 45 Mabey, D.G. *Measurements of Wing Buffeting on a Scimitar Model*, ARC CP 954, 1966.
- 46 Jones, J.G. *The Dynamic Analysis of Buffeting and Related Phenomena*, AGARD CP 102, November 1972.
- 47 Butler, G.F. Jones, J.G. RAE - unpublished. Note in preparation.
- 48 Cornette, E.S. *Wind Tunnel Investigation of the Effects of Wing Bodies, Fences, Flaps and Fuselage Addition on Wing Buffet Response of a Transonic Transport Model*, NASA TN D 637.
- 49 Jones, J.G. *Aircraft Dynamic Response Associated with Fluctuating Flow Fields*, AGARD Lecture Series 74, Aircraft Stalling and Buffeting, February 1975.
- 50 Mabey, D.G. Butler, G.F. *Measurements of Buffeting on Two 68° Delta Wings of Different Materials*, RAE TR 76-009, also AGARD Paper 6, Symposium on Air Frame Response to Transonic Flow, April 1977.
- 51 Rainey, A.G. Byrdsong, T.A. *An Examination of Buffeting Analysis based on Experiments with Wings of Varying Stiffness*, NASA TN D 3 (1959).
- 52 Polentz, P.P. Page, W.A. Levy, L.L. *The Unsteady Normal Force Characteristics of Selected NACA profiles at High Subsonic Mach Numbers*, NACA RM A 55 002, May 1955.
- 53 Stapleton, S.F. Pegram, B.V. *Comments on some Wind Tunnel and Flight Experience of Post-Buffet Behaviour of the Harrier Aircraft*, Paper 20A1, AGARD CP 187, April 1976.
- 54 Hanson, P.W. *Evaluation of an Aeroelastic Model Technique for Predicting Aircraft Buffeting Loads*, NASA TN D 7066, February 1973.
- 55 Moss, G.F. Pierce, D. *The Dynamic Response of Wings in Torsion at High Subsonic Speeds*, Paper 4, AGARD Symposium on Airframe Response to Unsteady Flow, April 1977.
- 56 Coe, C.F. Riddle, D.W. *Separated Flow Unsteady Pressures and Forces on Elastically Responding Structures*, Paper I, AGARD Symposium on Airframe Response to Unsteady Flow, April 1977.
- 57 Becker, J. Dau, K. *Evaluation of Vibration Levels at the Pilot Seat Caused by Wing Flow Separation*, Paper 5, AGARD Symposium on Airframe Response to Separated Flow, April 1977.
- 58 Kilgore, R.A. Adcock, J.B. Ray, E.J. *Flight Simulation Characteristics of the Langley High Reynolds Number Cryogenic Transonic Tunnel*, AIAA Paper 74-80, February 1974.
- 59 Mabey, D.G. *Some Remarks on Dynamic Aeroelastic Model Tests in Cryogenic Wind Tunnels*, NASA CR 145029, September 1975.
- 60 Boyden, R.P. *Preliminary Results of Buffet Tests in a Cryogenic Wind Tunnel*, NASA TM 81923.
- 61 Chapman, D.R. *Computational Aerodynamics, Development and Outlook*, AIAA J, Vol.17, No.10, p.1076-1083.
- 62 Levy, L.L. *An Experimental and Computational Investigation of the Steady and Unsteady Transonic Flow Fields about an Aerofoil in a Solid Wall Test Channel*, AIAA Paper 77-678, June 1977.

- 63 McDevitt, J.B. *Supercritical Flow About a Thick Circular Arc Aerofoil*, NASA TM 78549, January 1979.
- 64 Mabey, D.G.  
Welsh, B.L.  
Cripps, B.L. *Measured and Predicted Periodic Flows on a 14% Thick Biconvex Wing at Transonic Speeds*, RAE TR to be issued.

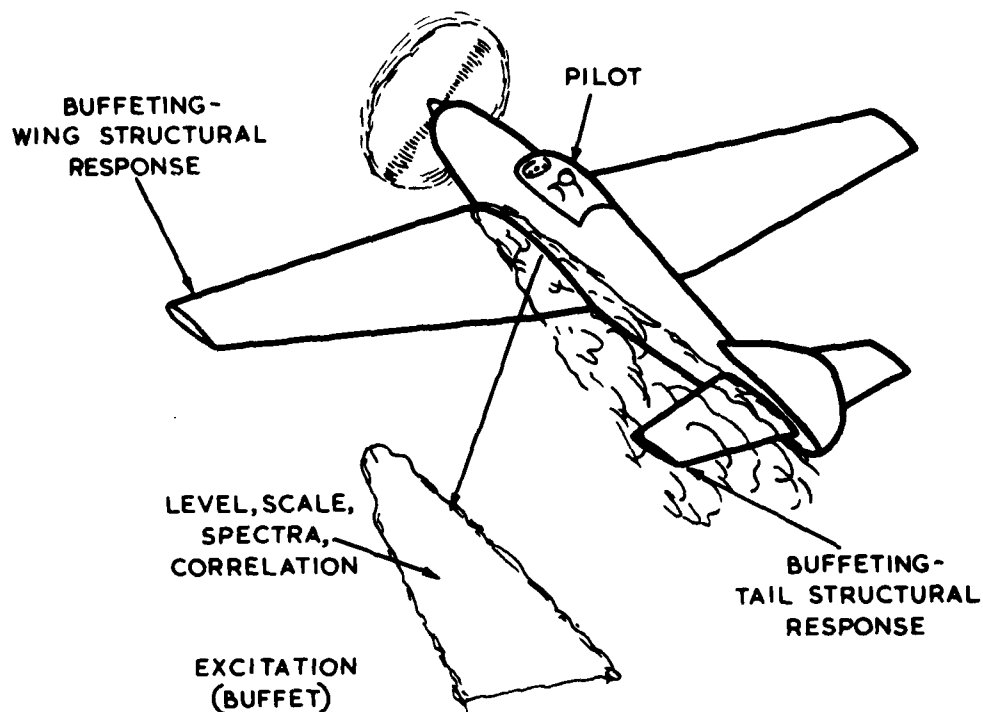


Fig 1 Buffeting

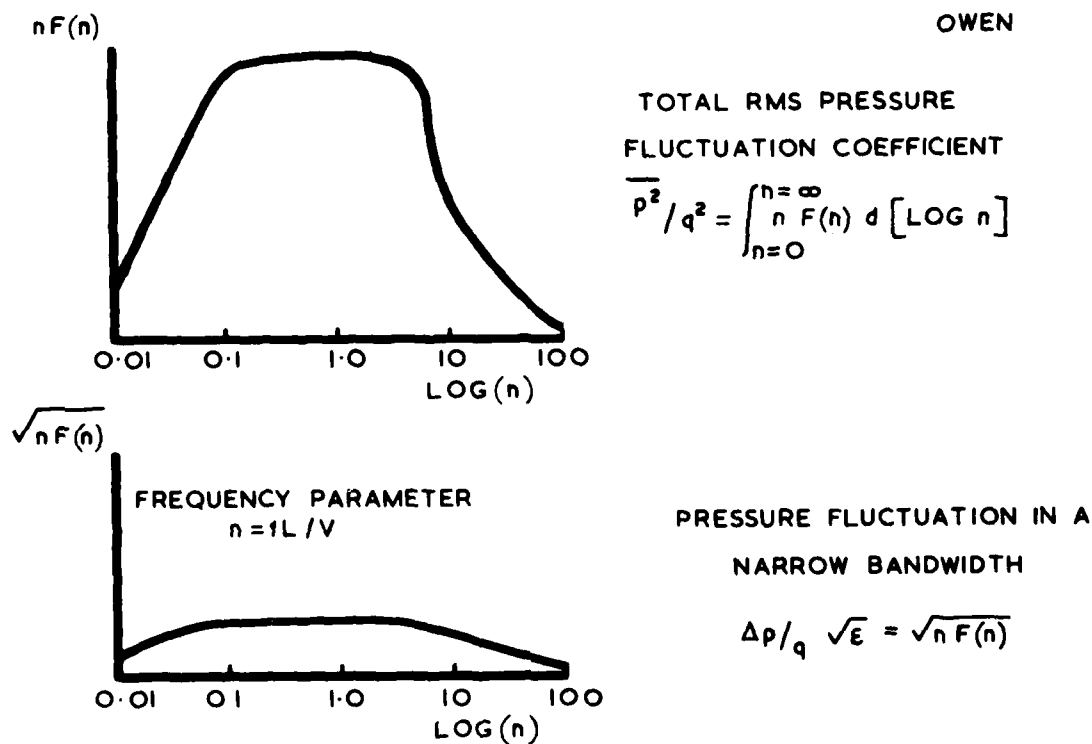


Fig 2 Dimensionless representation of excitation spectra

Figs 3&4

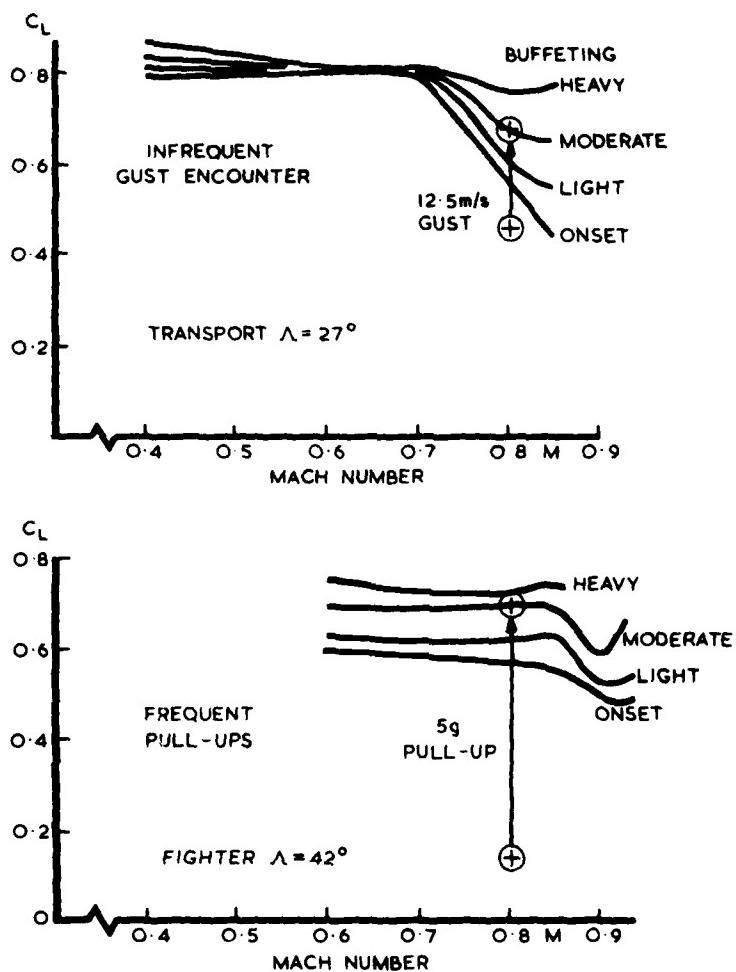


Fig 3 Buffeting criteria for transport and fighter aircraft

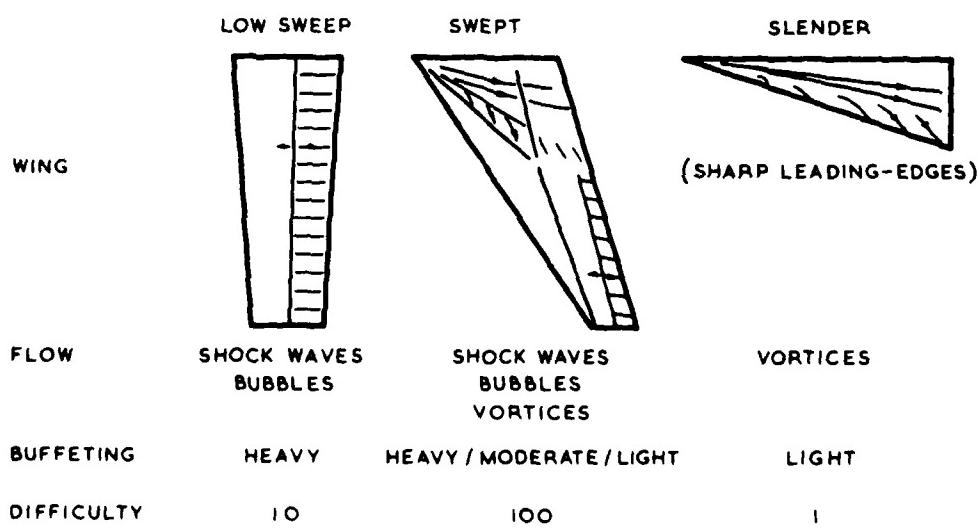


Fig 4 Classification of flows and associated buffeting

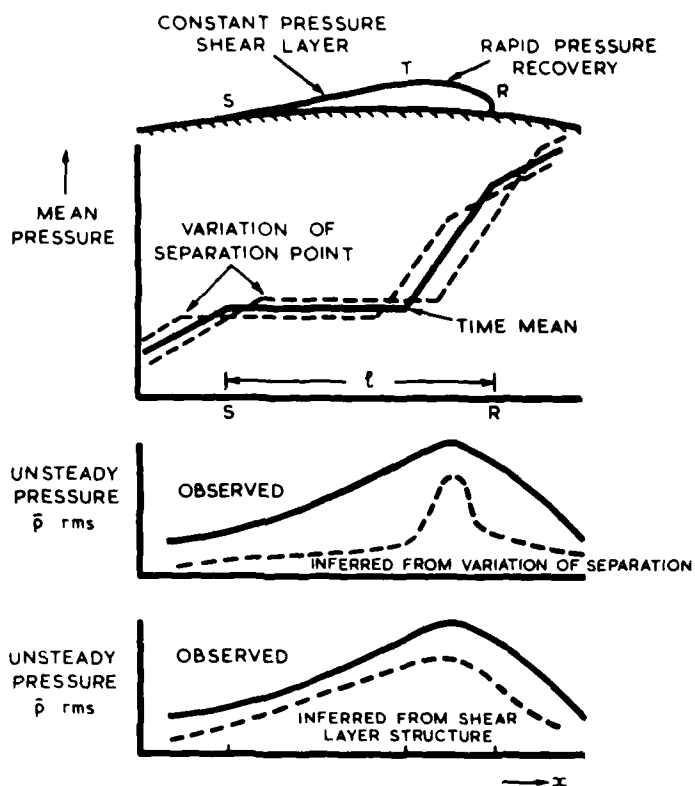


Fig 5 Mean flow and pressure fluctuations caused by separation bubbles

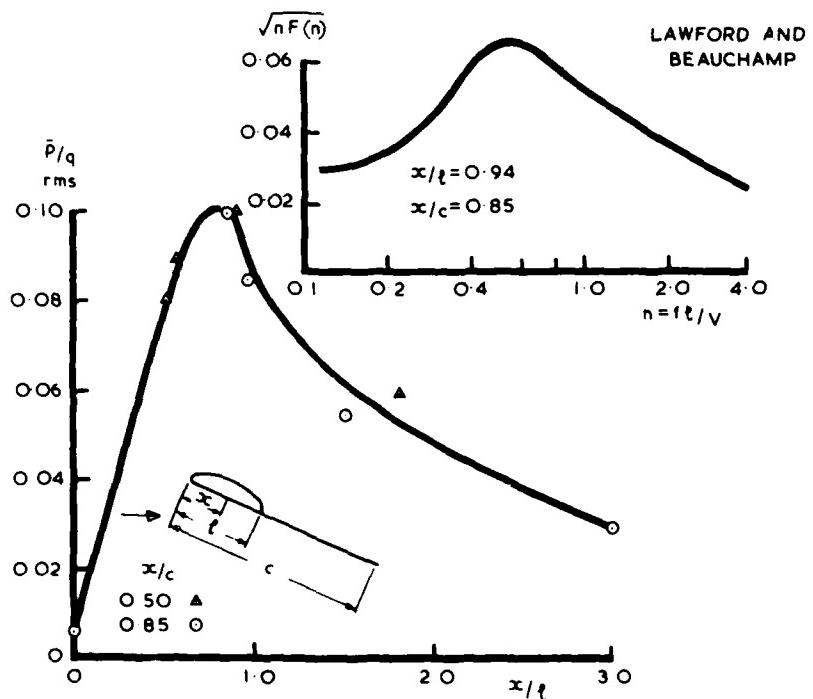


Fig 6a Excitation caused by leading-edge bubble,  $M = 0.14$

Figs 6b,7&8

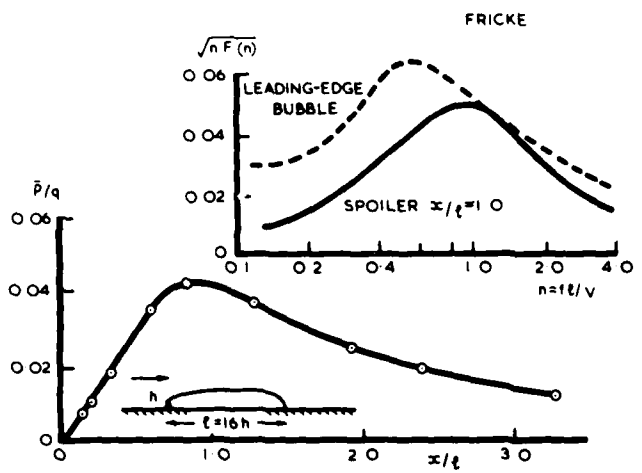


Fig 6b Excitation caused by a spoiler,  $M = 0.12$

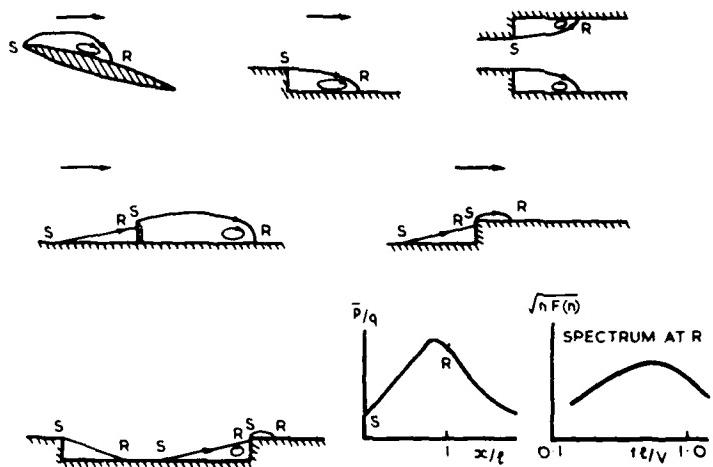


Fig 7 Types of bubble flow

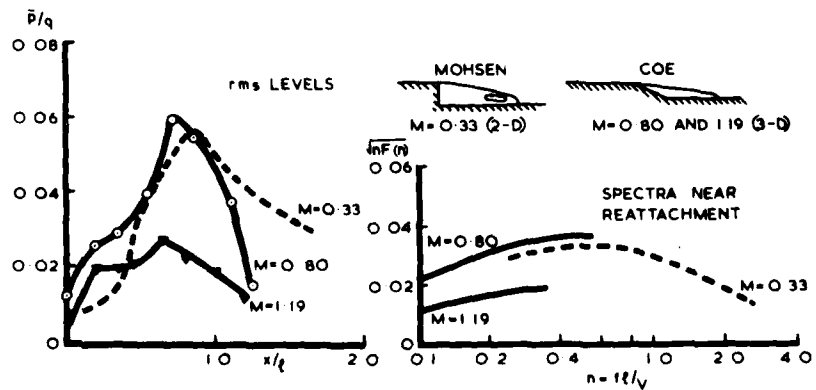


Fig 8 Comparison of excitation caused by the flow down a step at  $M = 0.33$ ,  $0.80$  and  $1.19$

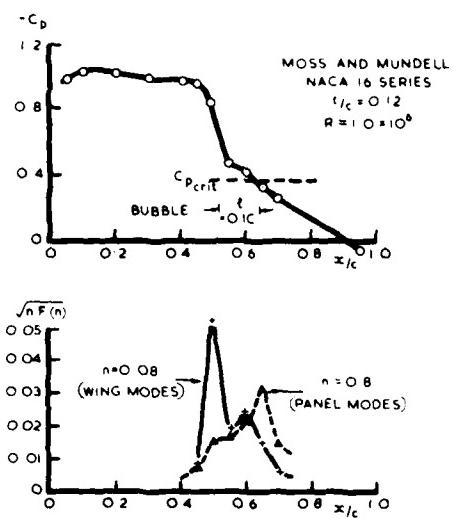


Fig 9 Excitation on an aerofoil near buffet onset,  $M = 0.82$ ,  $\alpha = 6.7^\circ$

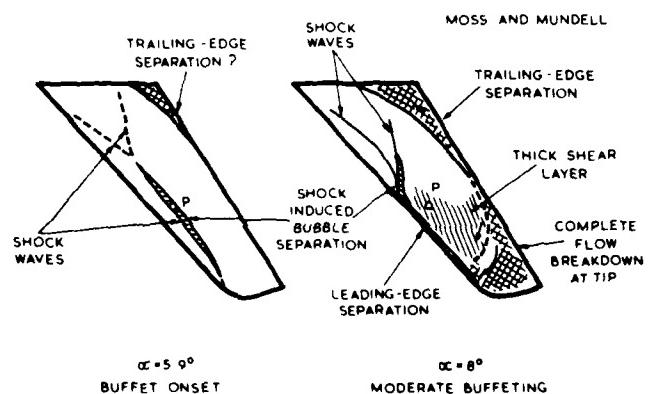


Fig 10 Transonic flow on a swept wing,  $M = 0.80$

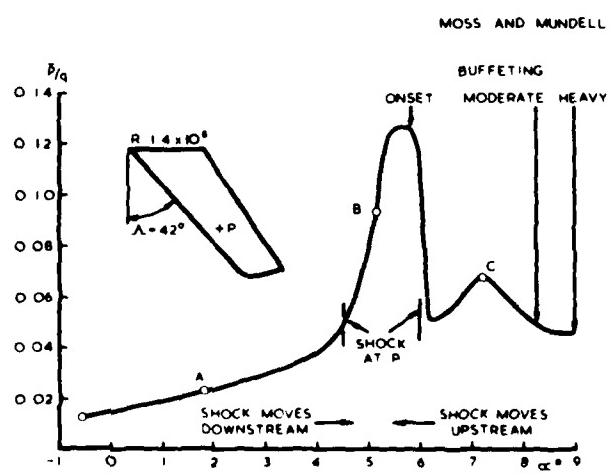


Fig 11 Excitation on a swept wing,  $M = 0.80$

Figs 12,13&14

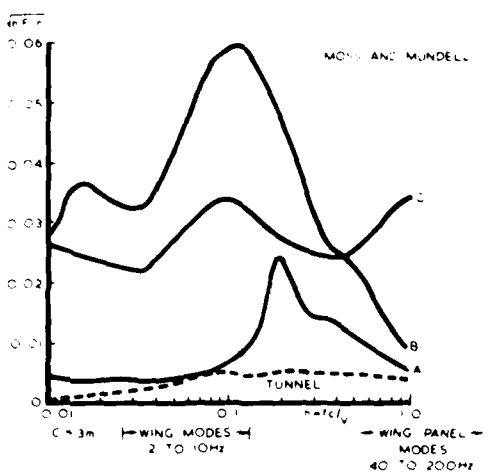


Fig 12 Spectra of excitation on a swept wing,  $M = 0.80$

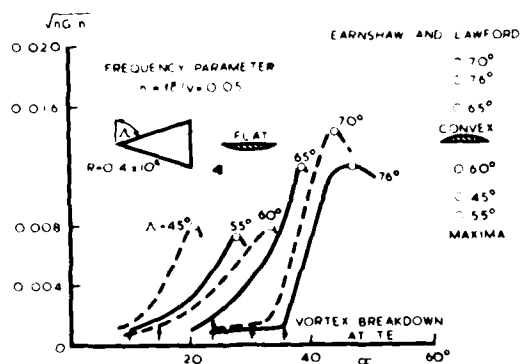


Fig 13 Variation of fluctuating normal force coefficient with incidence for delta wings  $M = 0.08$

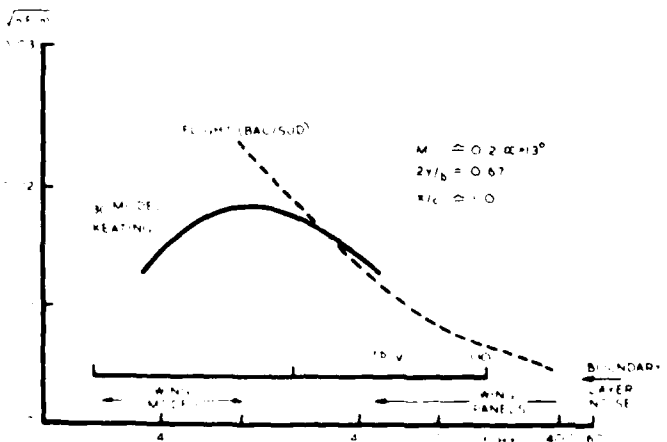


Fig 14 Low speed excitation on a slender wing

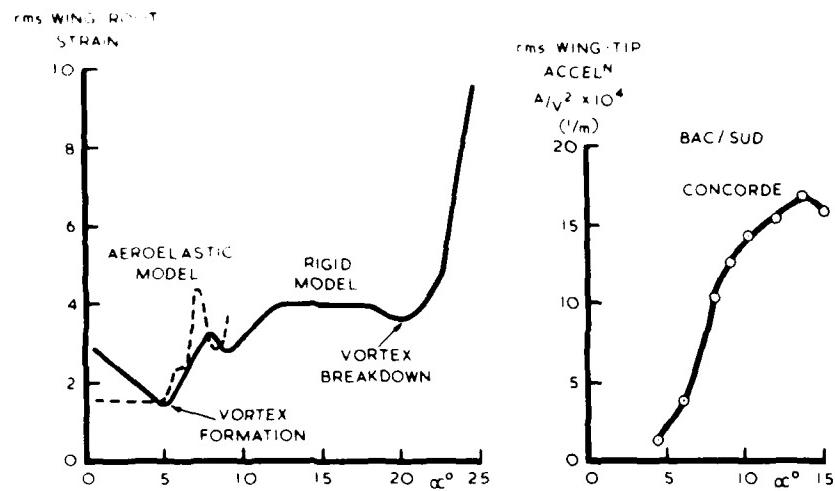


Fig 15 Light buffeting on slender wings,  $M = 0.2$

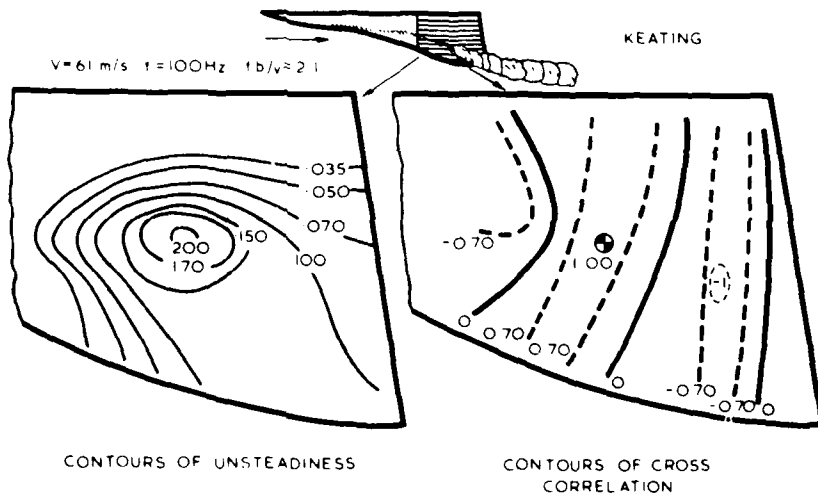


Fig 16 Excitation on BAC 221 at vortex breakdown  $\alpha = 21.5^\circ$ ,  $r = -3^\circ$ ,  $M = 0.2$

TM Str 980

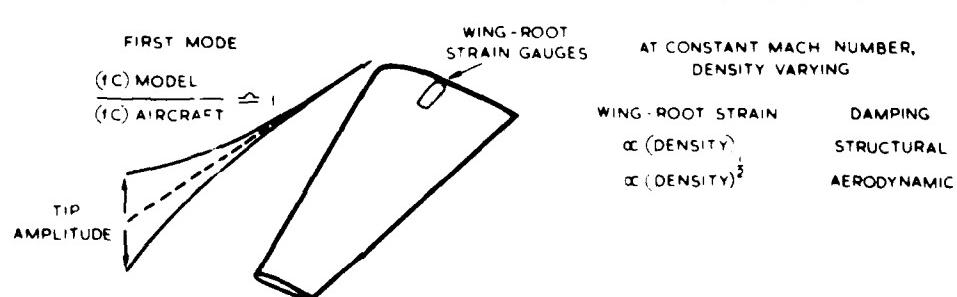


Fig 17 Similarity relations for buffeting

Figs 18&19

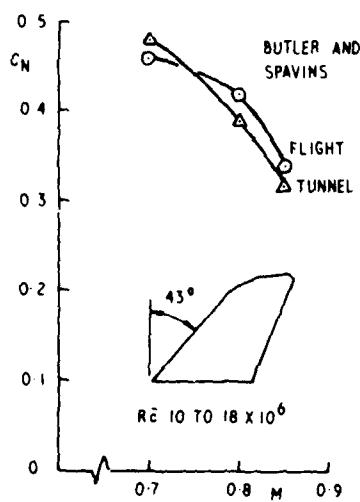


Fig 18 Flight/tunnel comparison for buffet onset on a small fighter aircraft

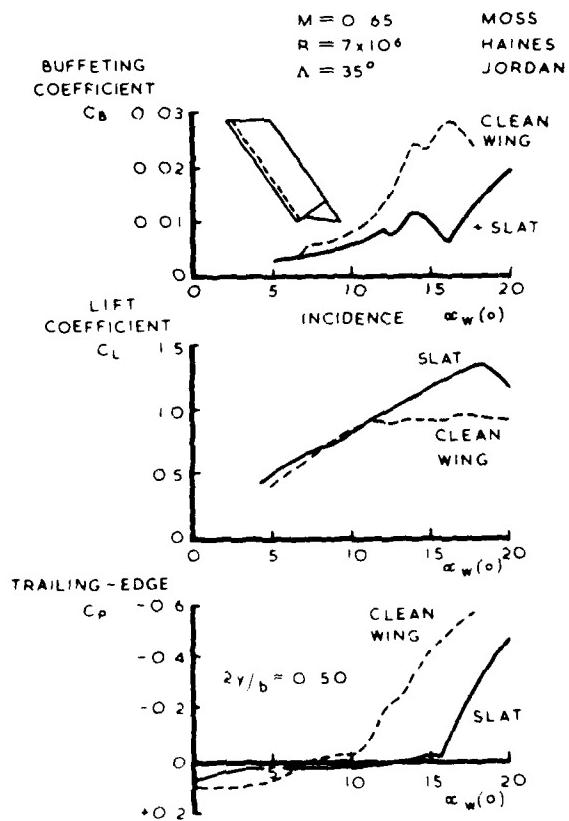


Fig 19 Influence of leading-edge slats on buffeting, forces and trailing-edge pressures

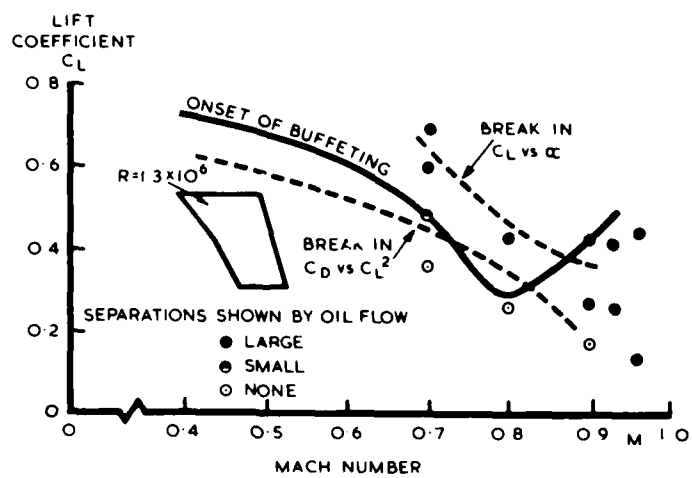


Fig 20 Derivation of flow separation boundaries

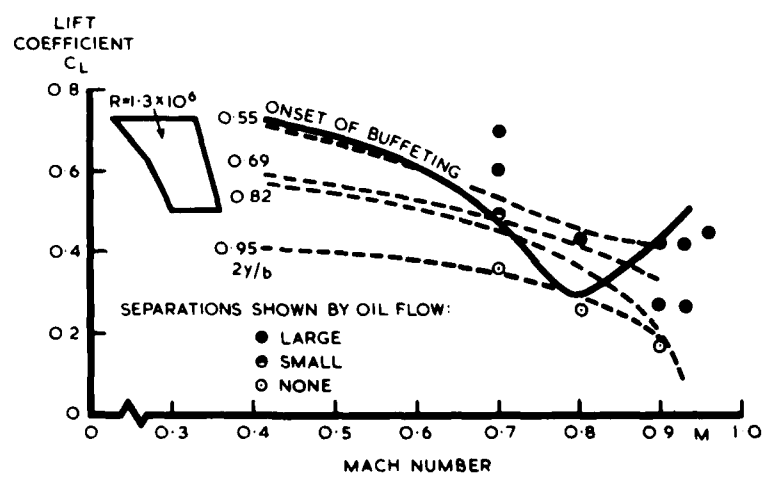


Fig 21 Boundaries of trailing-edge pressure divergence

Figs 22&23

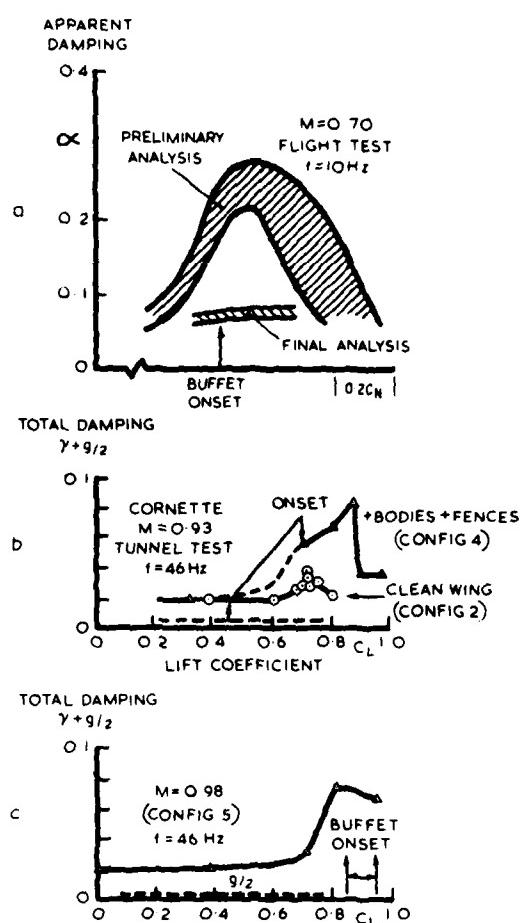


Fig 22 Variation of total damping with lift coefficient

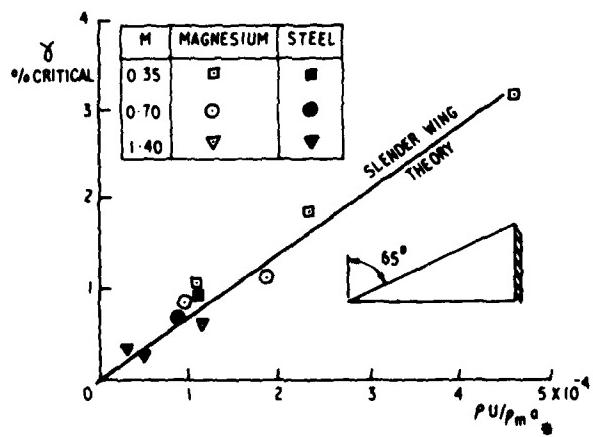


Fig 23 First bending mode - variation of aerodynamic damping with density and velocity

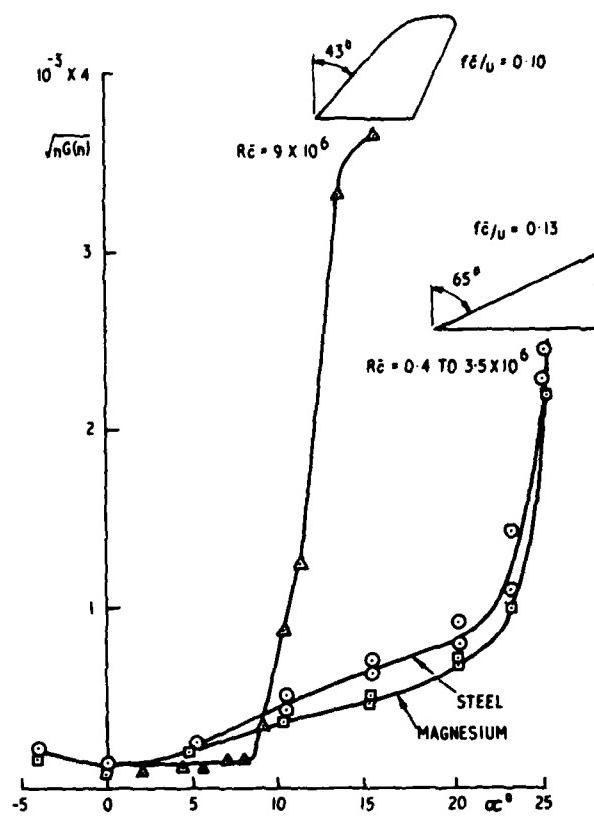


Fig 24 Buffet excitation parameter for two wings  $M = 0.70$

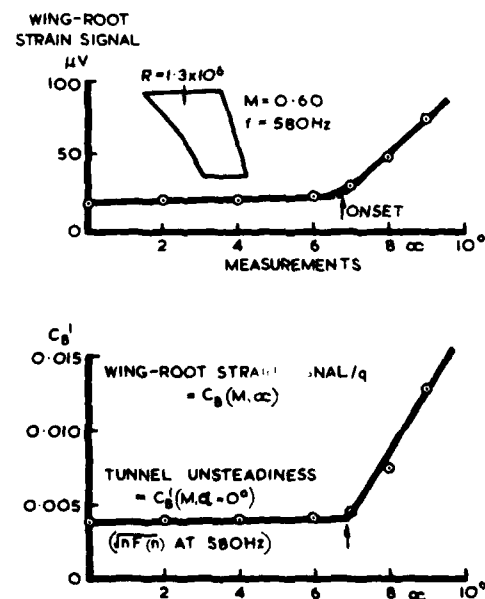


Fig 25 Definition of buffeting coefficients

Figs 26&27a&b

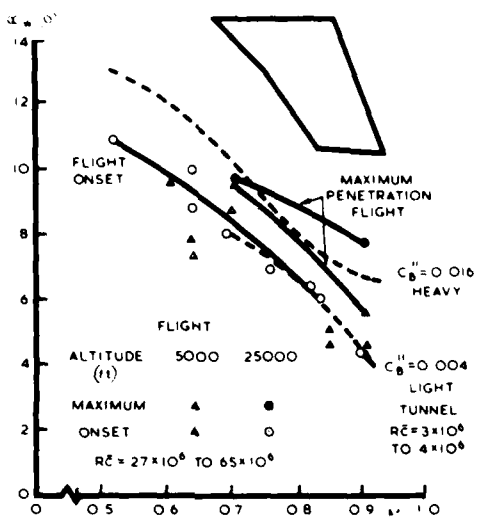
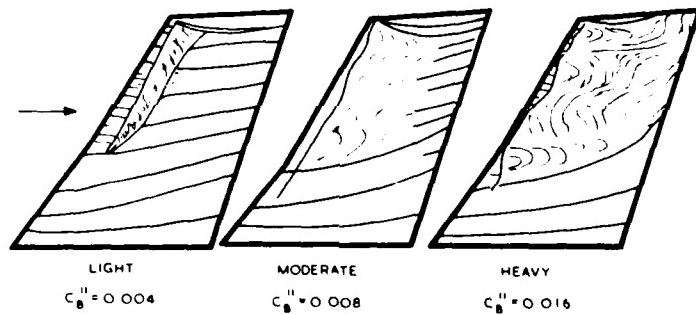
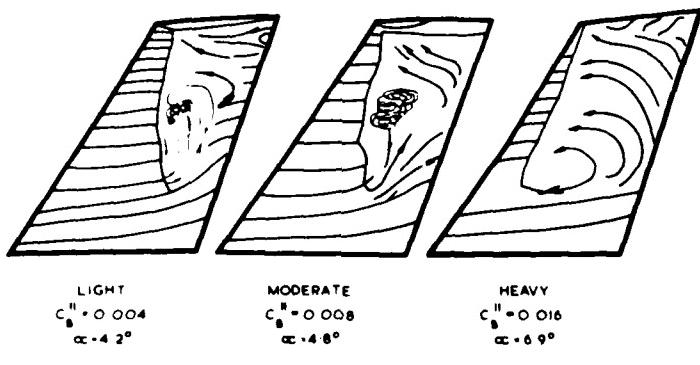


Fig 26 Aircraft buffeting penetration boundaries and model buffeting contours



$\alpha$   $M = 0.70$   $R = 4 \times 10^6$



$\alpha$   $M = 0.90$   $R = 4 \times 10^6$

Fig 27a&b Surface flow patterns at different levels of buffeting

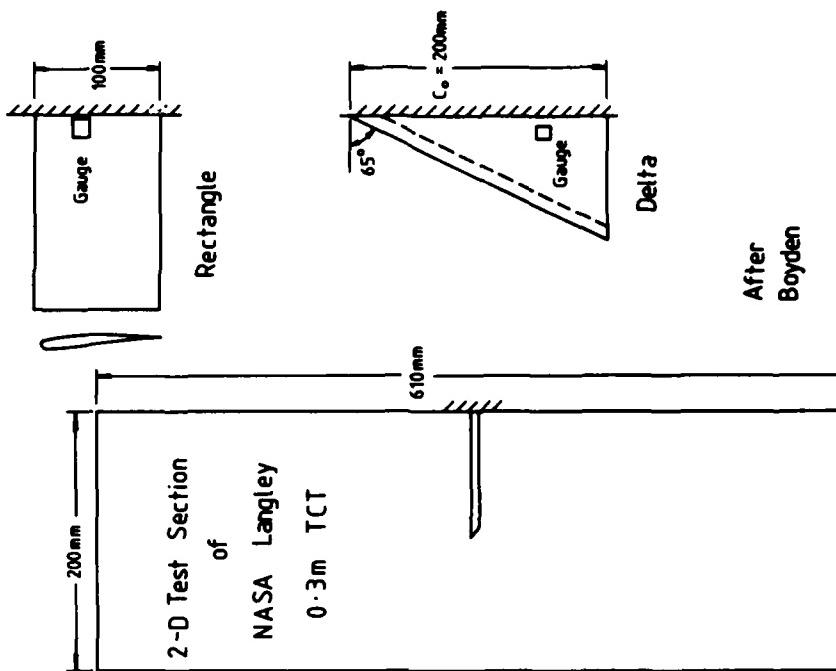


Fig 29 Wings for buffeting tests in Cryogenic tunnel

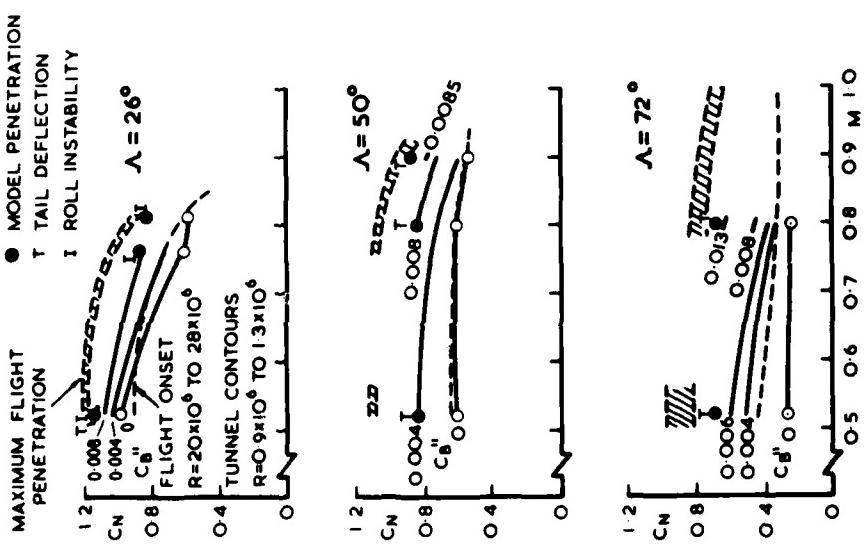


Fig 28 Variable geometry aircraft buffeting penetration boundaries and model buffeting contours

Figs 30&31

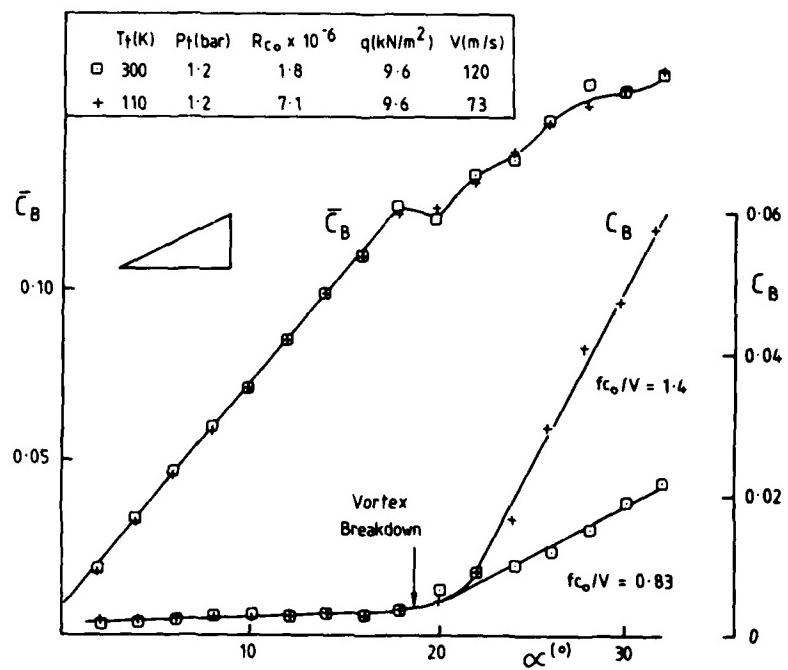


Fig 30 Negligible influence of Reynolds number  $M = 0.35$

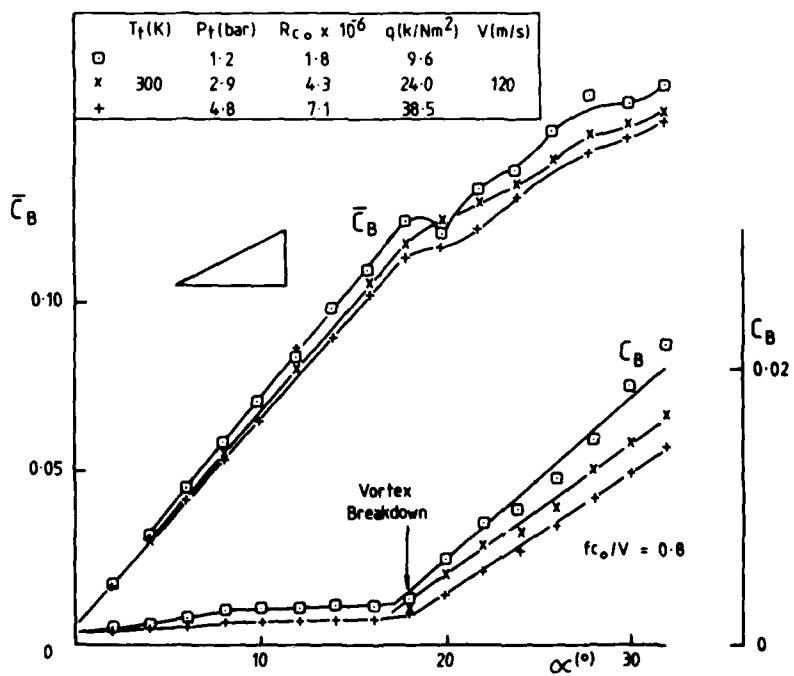


Fig 31 Influence of static aeroelastic distortion  $M = 0.35$

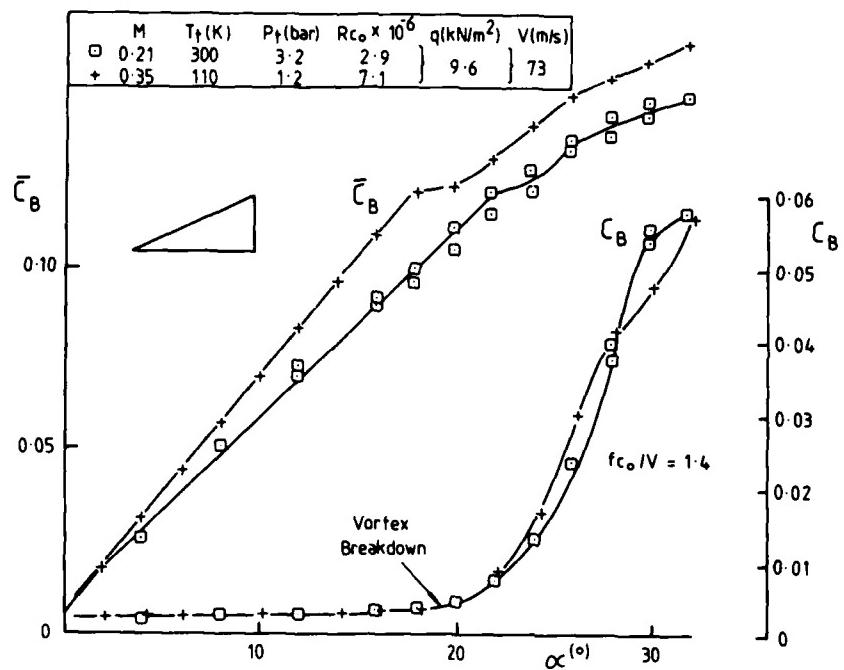


Fig 32 Influence of Mach number

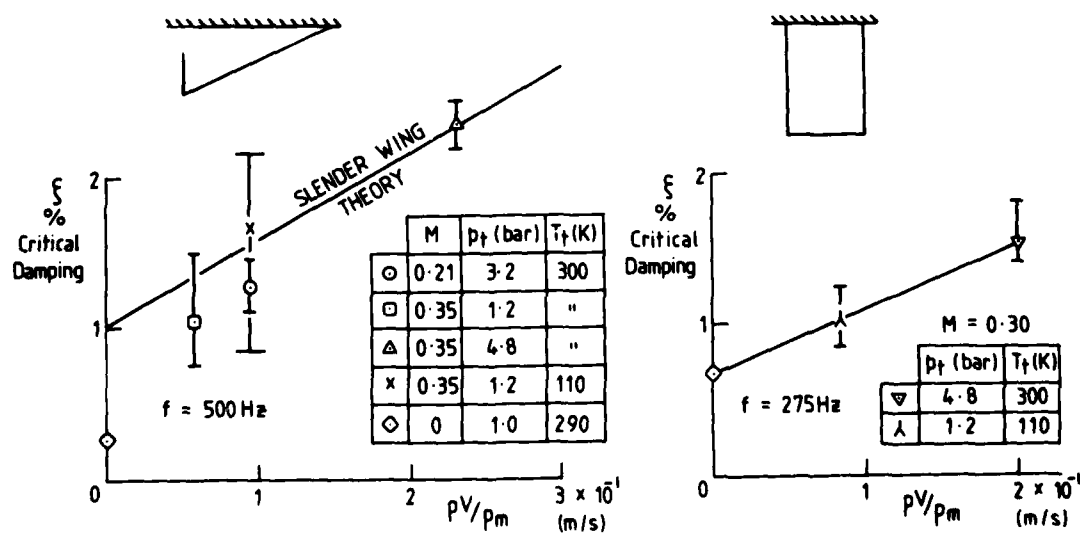


Fig 33 Preliminary damping measurements for buffeting tests in cryogenic wind tunnel

Figs 34&35

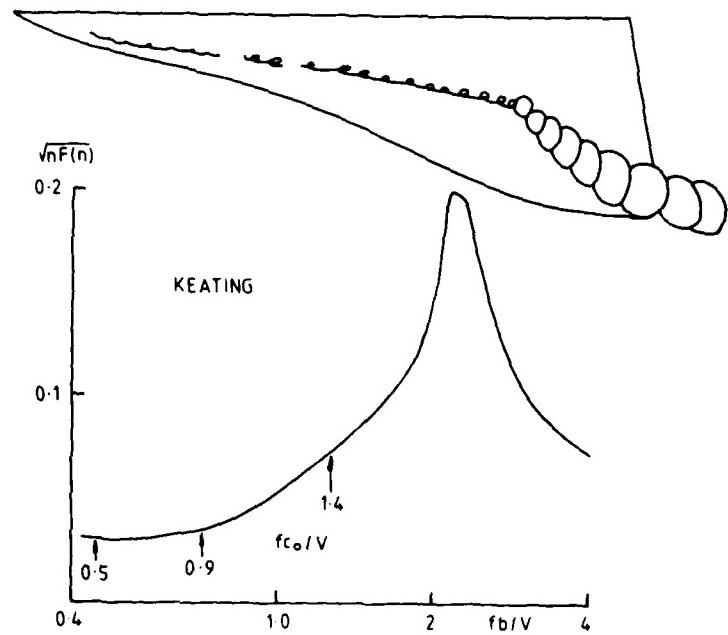


Fig 34 Spectrum at Vortex breakdown

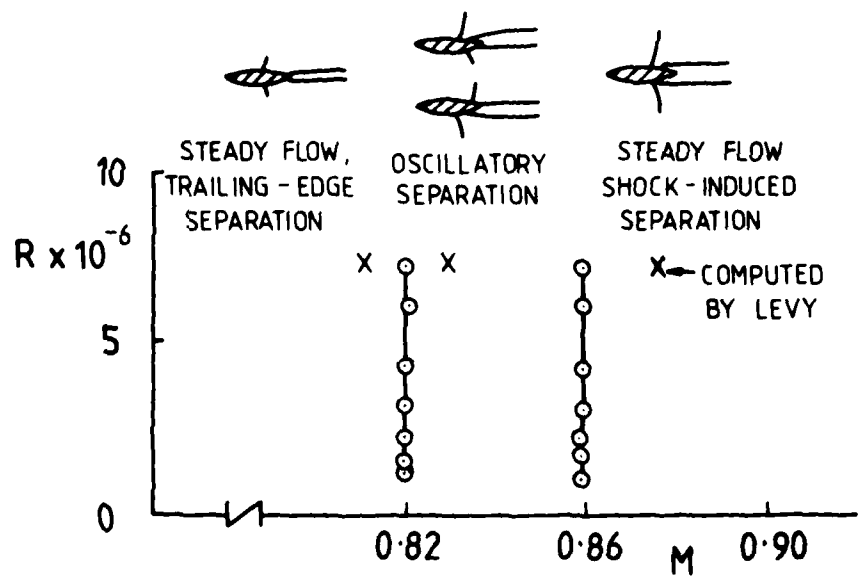


Fig 35 Flow domains for a 14% thick biconvex aerofoil  
 $\alpha = 0^\circ$  (fixed transition)

## REPORT DOCUMENTATION PAGE

Overall security classification of this page

UNLIMITED

As far as possible this page should contain only unclassified information. If it is necessary to enter classified information, the box above must be marked to indicate the classification, e.g. Restricted, Confidential or Secret.

1. DRIC Reference (to be added by DRIC)	2. Originator's Reference TM RAE Structures 980	3. Agency Reference N/A	4. Report Security Classification/Marking UNLIMITED
5. DRIC Code for Originator  850100	6. Originator (Corporate Author) Name and Location  Royal Aircraft Establishment, Farnborough, Hants, UK		
5a. Sponsoring Agency's Code  N/A	6a. Sponsoring Agency (Contract Authority) Name and Location  N/A		
7. Title Some remarks on buffeting			
7a. (For Translations) Title in Foreign Language			
7b. (For Conference Papers) Title, Place and Date of Conference AGARD LS "Unsteady airloads and aeroelastic problems in separated and transonic flows" in Brussels, March 1981			
8. Author 1. Surname, Initials Mabey, D.G.	9a. Author 2	9b. Authors 3, 4 ....	10. Date February 1981   Pages   Refs. 33   64
11. Contract Number N/A	12. Period N/A	13. Project	14. Other Reference Nos.
15. Distribution statement (a) Controlled by – (b) Special limitations (if any) –			
16. Descriptors (Keywords) Unsteady aerodynamics.		(Descriptors marked * are selected from TEST)	
17. Abstract  Buffeting is defined as the structural response to the aerodynamic excitation produced by separated flows. The aerodynamic excitation produced by bubbles, vortices and transonic flows is discussed.  Different buffeting criteria for the wings of fighter and transport aircraft are developed. Methods of predicting the onset and severity of buffeting are reviewed. Some typical examples are discussed, in which improvements in wing buffeting are compared with changes in mean force measurements.  The first buffeting measurements on ordinary models in a <u>cryogenic</u> wind tunnel are analysed. The measurements confirm that cryogenic tunnels can separate Reynolds number and aeroelastic effects. The frequency parameter must be correct on the model if the aerodynamic excitation does not have a flat spectrum, as at vortex breakdown on a slender wing.  The violent periodic flows at transonic speeds recently observed on thick bi-convex aerofoils are briefly reviewed and compared with solutions of the full Navier-Stokes equations.			